Formulation of fully covariant Quantum-Molecular Dynamics for an N-body system with scalar and vector potentials

Jiaxing Zhao, a,b Joerg Aichelin, c,d Elena Bratkovskaya e,a,b

- ^a Helmholtz Research Academy Hessen for FAIR (HFHF), GSI Helmholtz Center for Heavy Ion Research. Campus Frankfurt, 60438 Frankfurt, Germany
- ^bInstitute for Theoretical Physics, Johann Wolfgang Goethe Universität, Frankfurt am Main, Germany
- ^cSUBATECH, Université de Nantes, IMT Atlantique, IN2P3/CNRS, 4 rue Alfred Kastler, 44307 Nantes cedex 3, France
- ^d Frankfurt Institute for Advanced Studies, Ruth-Moufang-Strasse 1, 60438 Frankfurt am Main, Germany
- ^e GSI Helmholtzzentrum für Schwerionenforschung GmbH, Planckstrasse 1, 64291 Darmstadt, Germany

 $E ext{-}mail:$ jzhao@itp.uni-frankfurt.de, aichelin@subatech.in2p3.fr, E.Bratkovskaya@gsi.de

ABSTRACT: We present a fully covariant transport framework for Molecular Dynamics that enables a consistent description of the evolution of relativistic N-body systems. For the first time, we derive relativistic equations of motion incorporating both scalar and vector interactions within a manifestly covariant formulation. This approach addresses several fundamental issues in relativistic many-body dynamics: the implications of different choices of time-constraints, the emergence of the non-relativistic limit, the frame independence of the system's evolution, and the distinct dynamical roles of scalar and vector potentials. These aspects are investigated in detail for the scattering of two- and four-body systems, offering new insights into the consistency and physical interpretation of relativistic interactions in a covariant setting.

KEYWORDS: relativistic evolution; Dirac constraints; world line condition; time constraints.

| C | ontents | |
|--------------|---|----|
| 1 | Introduction | 1 |
| 2 | Basic concepts | 4 |
| | 2.1 Poincaré Group and algebra | 5 |
| | 2.2 Constraints and world line condition | 6 |
| 3 | Non-relativistic time evolution of N-body systems | 9 |
| 4 | Relativistic time evolution of two-body systems | 10 |
| | 4.1 Formal development of the time evolution equations with scalar and vector | |
| | potentials | 10 |
| | 4.2 Relation to the RQMD, UrQMD, and JAM | 13 |
| | 4.3 The non-relativistic limit | 15 |
| | 4.4 Different choices of time constraints | 17 |
| | 4.5 Numerical study of a two-nucleon system with scalar and vector interactions | 19 |
| | 4.5.1 The influence of the vector and scalar potentials | 21 |
| | 4.5.2 The frame-independence of the trajectories | 26 |
| 5 | Relativistic four-body evolution | 27 |
| | 5.1 Four-nucleon system | 29 |
| 6 | Relativistic N-body evolution | 31 |
| 7 | Summary | 32 |
| \mathbf{A} | Time constraints and relativistic kinematics | 33 |
| | A.1 Time constraints | 33 |
| | A.2 Standard derivation of relativisitic EoMs | 34 |
| В | Numerical method for computing the mechanical momentum and related | d |
| | derivatives | 35 |

1 Introduction

The description of the time evolution of interacting many-body systems of particles with relativistic velocities is a central problem across nuclear, hadronic, and particle physics. Whenever strongly interacting systems are created under extreme conditions—such as in heavy-ion collisions, astrophysical environments, or the early universe—their microscopic constituents evolve far from equilibrium while exchanging energy, momentum, and quantum

numbers. The challenge lies in bridging relativistic quantum field theory (QFT) with transport and kinetic approaches that remain tractable for many-body systems. At the most fundamental level, the evolution is governed by QFT, where fields interact according to the Lagrangian of the underlying theory. However, a direct solution of the full many-body QFT dynamics is not feasible except for very small systems.

Even in classical systems, the description of many-body dynamics poses formidable challenges, although such systems frequently occur in nuclear and astrophysical contexts. In nuclear physics, essentially two families of relativistic transport approaches have been developed: (a) the Boltzmann-Vlasov type, usually referred to as the Boltzmann-Uehling-Uhlenbeck (BUU) method, and (b) the molecular dynamics type, usually called the Quantum Molecular Dynamics (QMD) method. For detailed comparisons, we refer the reader to the comprehensive reviews in Refs. [1–10].

The BUU approach can be explicitly derived from the Bogoliubov-Born-Green-Kirkwood-Yvon (BBGKY) hierarchy by truncation at the two-body level. We mention that the formulation of many-body dynamics up to infinite order has been proposed in Refs. [4, 11] based on correlation dynamics within the cluster expansion method, however, the numerical solution of this bound equations are still out of power of modern computers, thus a truncation scheme has to be applied. The truncation procedure on the 2PI (2-particleirreducible) level leads to a transport equation for the one-body phase-space distribution function $f(\mathbf{r}, \mathbf{p}, t)$, which evolves under the influence of a mean-field potential and a collision integral describing two-body scattering, including Pauli blocking for fermions and Bose enhancement for bosons. Covariant formulations of BUU models exist [4, 6, 12], as well as its extension to $n \leftrightarrow m$ collision integrals [13]. Further development of the transport approach for the one-body phase-space distribution function has been presented in [14, 15] by the realization of a microscopic covariant off-shell dynamical approach PHSD (Parton-Hadron-String Dynamics) for strongly interacting systems, formulated as the first order gradient expansion [16, 17] of Kadanoff-Baym equations for Green's functions in phase-space representation. The BUU models are computationally efficient and well-suited for describing the time evolution of single-particle observables. However, the higher order correlations are lost due to the truncation. There are several flavors of BUU type transport approaches that incorporate relativistic features either through relativistic kinematics and/or by introducing a relativistic mean-field (RMF) potential. Representative implementations include pBUU [18], RVUU [19], RBUU [4], HSD [6], IBUU [20], GiBUU [21], SMASH [22], DJBUU [23], AMPT [24], and BAMPS [25].

The QMD approach, by contrast, follows a different philosophy. Instead of working with a phase-space distribution function, QMD models represent nucleons (or partons) as localized Gaussian wave packets whose centroids in coordinate and momentum space evolve according to a time-dependent variational principle [26, 27], supplemented by stochastic two-body scattering processes. This n-body framework allows to retain correlations beyond the mean-field level, including event-by-event fluctuations, cluster formation, and multifragmentation phenomena, which are conceptually not to capture within BUU-type models.

Using constrained Hamiltonian dynamics, the first fully relativistic version of QMD

was developed as RQMD [28–30], which constructed relativistic equations of motion with Lorentz-scalar interactions. Later JAM [31] has been advanced, which is based on the same theoretical approach and uses different approximations. Although not fully covariant, this approach has been applied to relativistic heavy-ion collisions [32–34]. Also UrQMD [35, 36] is a relativistic QMD approach, however, in numerical calculations it is mostly used in a cascade mode or with non-relativistic potentials. In addition, a relativistic QMD formulation based on the Nambu–Jona-Lasinio (NJL) model has been developed to describe the expansion and hadronization of a quark-antiquark plasma. In this framework, the NJL model generates a density- and time-dependent constituent mass, which effectively acts as a relativistic scalar potential [37].

Consequently, BUU and QMD approaches represent complementary strategies. BUU excels in computational efficiency and the description of bulk single-particle observables under a mean-field approximation, making it particularly suited for studying average properties of nuclear reactions. In contrast, QMD naturally incorporates correlations and fluctuations that play a crucial role in fragment production, event-by-event observables, and complex many-body dynamics. Together, these frameworks provide complementary insights and form the theoretical backbone of modern transport theory in nuclear physics.

In relativistic theories, there are two types of potentials: a scalar potential U_S , which is invariant under Lorentz transformations, and a vector potential V^{μ} , which transforms as a four-vector. The analysis of elastic proton–heavy-ion scattering data indicates that the absolute magnitudes of U_S and V^{μ} are of comparable order [38]. Moreover, the elementary nucleon–nucleon interaction, on which the nuclear relativistic mean-field (RMF) approach is based, naturally distinguishes between scalar and vector fields, which are associated with the different mesons exchanged between nucleons [39–42].

One of the primary goals of the upcoming relativistic heavy-ion experiments at RHIC-BESII, CBM, HIAF, and NICA is to provide insight in the hadronic equation of state (EoS) or more generally, in the phase structure of strongly interacting matter. The EoS depends on the baryon density and hence on the zero component of the current of the interacting baryons. For the study of relativistic heavy-ion collisions and the theoretical analysis of the experimental data it is therefore necessary to have a fully covariant transport approach, which includes both scalar and vector potentials and provides covariant equations of motion. These depend on the appropriate formulation of time constraints that preserve cluster separability.

The purpose of this paper is to develop such a framework. We derive relativistic transport equations for an interacting many-body system that are manifestly covariant and explicitly include both scalar and vector interactions. We follow the constraint Dirac dynamics approach in reducing the 8N dimensional phase space to 6N+1 dimensions using energy and time constraints. The latter connect the particle times, the zero components of the particle position 4-vector, with a Lorentz invariant parameter τ , which characterizes the position on the 6N+1 dimensional hypersurface. Depending on its definition, this parameter can be identified with the time in the non-relativistic limit. Formulating the evolution equation of the particle 4-vectors as a function of τ allows to move the particles in a covariant way, respecting the time (and energy) constraints. The individual particle

times, the zero component of the particle 4-vectors x^{μ} , can be recovered as a function of τ by exploiting the time constraints. This allows finally to calculate the particle trajectories $\mathbf{x}(t)$ and $\mathbf{p}(t)$. These are independent of the choice of the Lorentz frame in which the evolution equations are solved.

We demonstrate the frame independence of our approach by solving the equations of motion in two distinct Lorentz frames and separately investigate the influence of scalar and vector potentials on particle trajectories. We begin with a systematic overview and clarification of several fundamental concepts in relativistic dynamics. Subsequently, we derive the equations of motion for two- and many-body systems and compare with different formulations proposed in earlier relativistic QMD approaches, with particular attention to their underlying assumptions.

The structure of the paper is as follows. In Section 2, we introduce the basic concepts of the relativistic dynamical framework, including dynamical constraints, Poincaré transformations, world-line invariance, Dirac brackets, and related topics. The non-relativistic limit of an interacting N-body system is presented in Section 3. Section 4 is devoted to the derivation of the relativistic two-body evolution equations, where we discuss key issues such as the role of time constraints and how it approaches the non-relativistic limit. The frameworks for four-body and general N-body systems are presented in Sections 5 and 6, respectively. Finally, we summarize our findings in Section 7.

2 Basic concepts

There is a long history of research on relativistic particle dynamics [43]. A major milestone was Dirac's pioneering formulation of constrained Hamiltonian dynamics [43], which provided a systematic framework for incorporating relativistic invariance into dynamical systems. Building on this foundation, important extensions were developed by Komar [44, 45], Samuel [46, 47], Sudarshan, Mukunda, and Goldberg [48], and Todorov [49], who generalized the formalism to relativistic two- and many-body systems and analyzed different choices of constraints.

A further development towards a numerically tractable transport approach has been advanced by Sorge, Stöcker, and Greiner [28, 50], who laid the groundwork for relativistic quantum molecular dynamics. In this approach they used a scalar potential, which is a function of the scalar density, to describe the interaction among nucleons. This interaction cannot be related to an equation of state, which is a function of the baryon density, the zero component of the 4- vector of the baryon current. Later Faessler and collaborators [29, 30, 51] published an independent but very similar method. More recently Aichelin and Marty [37] developed further this method to describe the time evolution of a quark - antiquark plasma based on the Nambu Jona-Lasinio Lagrangian. The latest in this series of models is that of Nara [33, 34], which employs vector potentials, however in an non-covariant approximate way.

In this section, we provide a systematic overview of these developments, tracing the evolution of relativistic dynamical frameworks from their fundamental theoretical origins to modern implementations in transport and molecular dynamics models.

2.1 Poincaré Group and algebra

We start out with a review of the common features and basic requirements of a relativistic theory. Starting point is the relativistic extension of the Poisson brackets

$$\{A,B\} \equiv \sum_{k=1}^{N} \left(\frac{\partial A}{\partial q_{k}^{\mu}} \frac{\partial B}{\partial p_{k,\mu}} - \frac{\partial A}{\partial p_{k}^{\mu}} \frac{\partial B}{\partial q_{k,\mu}} \right). \tag{2.1}$$

for position and momentum four-vectors, q^{μ} , p^{μ} , with $\mu = 0, ..., 3$. It's easy to check that the position and momentum four-vectors of each particle satisfy the Poisson brackets,

$$\begin{aligned}
\{q_i^{\mu}, q_j^{\mu}\} &= \{p_i^{\mu}, p_j^{\mu}\} = 0, \\
\{q_i^{\mu}, p_i^{\nu}\} &= \delta_{ij} g^{\mu\nu},
\end{aligned} (2.2)$$

with $g^{\mu\nu}$ being the Minkowski metric with the diagonal $\{1, -1, -1, -1\}$ and zero otherwise.

A relativistic theory has to be invariant under Lorentz transformations Λ and spacetime translations a. Both transformations form the Poincaré group with the group element, $R(\Lambda, a)$. Its action on the position vector is given by

$$R(\Lambda, a): \quad q'^{\mu} = R(\Lambda, a)q^{\mu} = \Lambda^{\mu}_{\nu}q^{\nu} + a^{\mu}.$$
 (2.3)

Finite transformations can be built with help of the infinitesimal ones. The algebra associated with the continuous symmetry group is given by the algebra of the generators of infinitesimal transformations. For a N-particle system, generators for the translation group and for the Lorentz group can be expressed as,

$$P_{\mu} = \sum_{n} p_{n,\mu},$$

$$M_{\mu\nu} = \sum_{n} q_{n,\mu} p_{n,\nu} - q_{n,\nu} p_{n,\mu}.$$
(2.4)

These ten generators respect the algebra of the group, which is called Poincaré algebra, which satisfies the Poisson brackets:

$$\{P_{\mu}, P_{\nu}\} = 0,
 \{M_{\mu,\nu}, P_{\rho}\} = g_{\mu\rho}P_{\nu} - g_{\nu\rho}P_{\mu},
 \{M_{\mu,\nu}, M_{\rho,\sigma}\} = g_{\mu\rho}M_{\nu\sigma} - g_{\mu\sigma}M_{\nu\rho} - g_{\nu\rho}M_{\mu\sigma} + g_{\nu\sigma}M_{\mu\rho}.$$
(2.5)

The generator of the Poincaré group is given by the combination of that of the Lorentz transformation and of a translation,

$$G \equiv a^{\mu}P_{\mu} + \frac{1}{2}\omega^{\mu\nu}M_{\mu\nu} \tag{2.6}$$

with the infinitesimal translation parameter a^{μ} and infinitesimal Lorentz transformation parameter $\omega^{\mu\nu}$. For a infinitesimal Poincaré transformation, the space-time coordinates of the same event in frame O and O' can be expressed using the Poisson bracket,

$$q'^{\mu} = q^{\mu} + \{q^{\mu}, G\} = q^{\mu} + \omega^{\mu}_{\nu} q^{\nu} + a^{\mu}, \tag{2.7}$$

where q^{μ} and q'^{μ} are four vectors in the frames O and O', respectively.

2.2 Constraints and world line condition

Relativistic theories are based on four-vectors whose transformation between two inertial systems is given by elements of the Poincaré group. As a consequence, the phase space of an N-particle system has no longer 6N dimensions as in non-relativistic dynamics but 8N. However, the physical phase-space trajectories have 6N+1 dimensions, which are the positions and momenta of the particles as a function of a evolution parameter τ , which is called the computational time. Thus we need constraints to reduce the number of degrees of freedom of the relativistic phase space.

The constraints concern those variables, which do not appear in the equation of particle trajectories, Usually N-constraints express the on-shell conditions (also called first class constraints) [44, 45], which read for free particles as $H_i = p_{i,\mu}p_i^{\mu} - m_i^2$. We can see that these constraints satisfy the Poisson bracket, $\{H_i, H_j\} = 0$ as well as the Poincaré invariance, $\{H_i, G\} = 0$. With the constraints H_i , the 8N-dimensional space reduces to a 7N dimensional hypersurface Σ . Because the H_i are Poincaré invariant, the 7N dimensional hypersurface Σ is also Poincaré invariant. One reduces the number of degrees of freedom further by introducing additional N-constraints χ_i (also called second class constraints), where N-1 constraints serve to pick a one-dimensional line on each sheet by fixing the relation between the time components of the N four-vectors in coordinate space. The last constraint connects these fixed time components with τ (in this paper, τ is not the proper time), the parameter, which characterizes the trajectory in the 6N dimensional phase space.

The selection of the second-class time constraints is not unique. The consequences of different choices has been discussed in many previous works [46–48]. The time constraints are chosen to fulfill the world line invariance. Given an initial value in the physical phase space one can solve the equation of motion (EoM) to get the corresponding phase space trajectory in a Minkowski space. This determines the world lines of all particles. Each point of a particle world line is a space-time event that can be Poincaré transformed according to the geometric standard rules of the Poincaré group. World line invariance means that the Poincaré-transformed particle world lines are the same as those that can be constructed by projecting the phase space trajectory on the Minkowski space after applying the canonical Poincaré transformation on the phase space variables. To clarify this concept, the concept of the Dirac bracket is introduced [43]. It is a generalization of the Poisson bracket developed by Dirac and used to describe the time evolution of any function of the phase-space variables along the trajectory determined by the constraints φ_i (including the first class H_i and second class χ_i). The definition of the Dirac bracket for any two phase-space functions A and B is

$$\{A, B\}^* \equiv \{A, B\} - \sum_{i,j}^{2N} \{A, \varphi_i\} C_{ij} \{\varphi_j, B\},$$
 (2.8)

with $C_{ij}^{-1} = \{\varphi_i, \varphi_j\}.$

One can easily arrive at the conclusion that the Dirac brackets yield the same result as the Poisson brackets (2.5) for the ten generators of the Poincaré group (2.4). Therefore we can also use the Dirac brackets to construct a transformation between the two inertial

systems O and O'. This transformation is noted as $R^*(\Lambda, a)$. Both transformations, $R(\Lambda, a)$ as well as $R^*(\Lambda, a)$, map the hypersurface Σ to Σ , but $R(\Lambda, a)$ and $R^*(\Lambda, a)$ map the same point in the frame O to different points in frame O', which both conserved all constraints. Because $\{\chi_i, G\}^* = 0$, χ_i is unchanged under a transformation $R^*(\Lambda, a)$ and the Dirac brackets transform a phase-space point on O to a phase-space point on O', which has the same value of τ . For the transformation using Poisson brackets this is generally not the case [52]. Therefore, Dirac brackets are the proper tool for dealing with transformations between two inertial frames.

Now, let us take the one body case as an example to see the condition of the World line invariance. For one free particle, the on-shell constraint is,

$$H = p_{\mu}p^{\mu} - m^2. \tag{2.9}$$

This constraint reduces the phase space from eight to seven dimensions by relating the energy of the particle with its three-momentum. The EoM in phase space on which this constraint is satisfied is given by the solution of,

$$\frac{dq^{\mu}}{d\tau} = \lambda \{q^{\mu}(\tau), H\},
\frac{dp^{\mu}}{d\tau} = \lambda \{p^{\mu}(\tau), H\},$$
(2.10)

where λ is a free parameter, which can be fixed by the second order constraint χ . This time constraint χ has been chosen quite differently what gives different equations of motion. The preservation of the constraint χ in τ gives,

$$\frac{d\chi}{d\tau} = \frac{\partial\chi}{\partial\tau} + \lambda\{\chi, H\} = 0, \tag{2.11}$$

and consequently,

$$\lambda = -\frac{\partial \chi}{\partial \tau} \{\chi, H\}^{-1}. \tag{2.12}$$

Applying this to the above EoM, we get

$$\frac{dq^{\mu}}{d\tau} = -\frac{\partial \chi}{\partial \tau} \frac{\{q^{\mu}, H\}}{\{\chi, H\}},$$

$$\frac{dp^{\mu}}{d\tau} = -\frac{\partial \chi}{\partial \tau} \frac{\{p^{\mu}, H\}}{\{\chi, H\}}.$$
(2.13)

Assuming O and O' are two inertial frames related by an infinitesimal element of the Poincaré group. The transformation can be realized with the Poisson bracket (where τ is not conserved), as given by equation Eq. (2.7) for a small time step $\delta \tau$,

$$q'^{\mu}(\tau) = q^{\mu}(\tau + \delta\tau) + \{q^{\mu}(\tau + \delta\tau), G\},$$

$$\approx q^{\mu}(\tau) + \frac{dq^{\mu}}{d\tau}\delta\tau + \{q^{\mu}(\tau), G\}.$$
(2.14)

This is called geometrical transformation. With the EoM (2.13), the q'^{μ} can be further expressed as,

$$q'^{\mu}(\tau) = q^{\mu}(\tau) - \frac{\partial \chi}{\partial \tau} \frac{\{q^{\mu}, H\}}{\{\chi, H\}} \delta \tau + \{q^{\mu}(\tau), G\}.$$
 (2.15)

On the other hand, the transformation between the inertial frames O and O' can be realized by $R^*(\Lambda, a)$, which is expressed using the Dirac bracket,

$$q'^{\mu}(\tau) = q^{\mu}(\tau) + \{q^{\mu}(\tau), G\}^*$$

$$= q^{\mu}(\tau) + \{q^{\mu}(\tau), G\} - \frac{\{q^{\mu}, H\}\{\chi, G\}}{\{H, \chi\}}.$$
(2.16)

This equation is called a canonical transformation to distinguish it from the geometrical transformation. The last step of the above equation is fulfilled due to $\{H,G\}=0$, as obtained before.

Comparing Eq. (2.15) with Eq. (2.16), we find that if

$$\delta \tau = \{\chi, G\} \left(\frac{\partial \chi}{\partial \tau}\right)^{-1}.$$
 (2.17)

is fulfilled, the transformation between two inertial systems using Dirac brackets (the canonical transformation) becomes identical to that using Poisson brackets (the geometrical transformation). This means that the world lines of particles remain the same under the two transformations. They are therefore frame independent. This requirement of frame independence of the trajectories is called the world line condition.

Time constraints, which can be chosen differently, have to fulfill Eq. (2.17) to be eligible for a relativistic dynamics. If they respect this equation they guaranty the World line invariance. Extending this to the N-body case we find

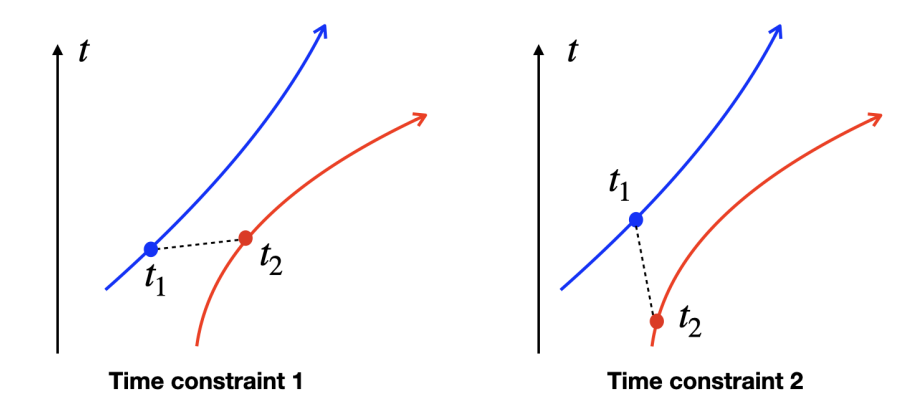


Figure 1. The sketch of the two particle system with different kinds of time constraints. The blue and red curves are trajectories of particle 1 and 2, respectively.

$$\delta \tau_i = \{\chi_i, G\} \left(\frac{\partial \chi_i}{\partial \tau}\right)^{-1}, \quad i = 1, ..., N.$$
 (2.18)

A simple way to choose the time constraints is to let N-1 of them be independent of τ (that means $\frac{\partial \chi_i}{\partial \tau} = 0$) and to demand Poincaré invariance, $\{\chi_i, G\} = 0$ for i = 1, ..., N-1. The last time constraint is τ -dependent and satisfies the world line invariance condition (2.17). However, there are many choices of time constraints that satisfy the above requirements. Different time constraints result in different equations of motion (EoM) and evolution times τ [37, 48]. These different time constraints connect different points in Minkowski space, as shown in Fig. 1. For a given τ the time constraints allow to determine the time component of the position four-vector of each of the particles. The independence of the physical trajectory from the choice of time constraints will be demonstrated in the next section for the two-body case through numerical calculations, and in the Appendix A for the one-body free case.

3 Non-relativistic time evolution of N-body systems

To compare the relativistic with the non-relativistic trajectories, we first examine the non-relativistic framework. The canonical momentum \mathbf{p}_i is the conjugated variable to the position, the mechanical momentum \mathbf{p}_i^* is the momentum, which is changed by the forces. In the non-relativistic case, the total Hamiltonian of an N-body system that interacts with a four-potential $A_{ij}^{\mu} = (A_{0,ij}, -\mathbf{A}_{ij})$ (analogous to a electromagnetic potential) and an additional scalar potential V_{ij} can be expressed as,

$$H = \sum_{i}^{N} \left[\frac{1}{2m_i} (\mathbf{p}_i - \mathbf{A}_i)^2 + A_{0,i} \right] + \sum_{i < j} V_{ij}, \tag{3.1}$$

where $\mathbf{A}_i = \sum_{i < j} \mathbf{A}_{ij}$ and $A_{0,i} = \sum_{i < j} A_{0,ij}$ is the common action of all other particles on particle i. The mechanical momentum \mathbf{p}_i^* is related to the canonical momentum \mathbf{p}_i , via e.g. $\mathbf{p}_i^* \equiv \mathbf{p}_i - \mathbf{A}_i$. Following the Hamilton-Jacobi approach, the equations of motion can be expressed by the non-relativistic Poisson equations as

$$\frac{d\mathbf{q}_{i}}{dt} = \frac{\partial H}{\partial \mathbf{p}_{i}} = \sum_{j=1}^{N} \left[\frac{\mathbf{p}_{j}^{*}}{m_{j}} \frac{\partial \mathbf{p}_{j}^{*}}{\partial \mathbf{p}_{i}} + \frac{\partial A_{0,j}}{\partial \mathbf{p}_{i}} \right],$$

$$\frac{d\mathbf{p}_{i}}{dt} = -\frac{\partial H}{\partial \mathbf{q}_{i}} = -\sum_{j=1}^{N} \left[\frac{\mathbf{p}_{j}^{*}}{m_{j}} \frac{\partial \mathbf{p}_{j}^{*}}{\partial \mathbf{q}_{i}} + \frac{\partial A_{0,j}}{\partial \mathbf{q}_{i}} \right] - \sum_{j \neq i} \frac{\partial V_{ij}}{\partial \mathbf{q}_{i}}.$$
(3.2)

Now, let's check the time derivative of the mechanical momentum and the "Lorentz-like" force,

$$\frac{d\mathbf{p}_{i}^{*}}{dt} = \frac{d\mathbf{p}_{i}}{dt} - \frac{\partial \mathbf{A}_{i}}{\partial t} - \sum_{j=1}^{N} (\dot{\mathbf{q}}_{j} \cdot \nabla_{j}) \mathbf{A}_{i}$$

$$= \sum_{j=1}^{N} (\mathbf{v}_{j} \nabla_{i} \mathbf{A}_{j} - \nabla_{i} A_{0,j}) - \sum_{j \neq i} \nabla_{i} V_{ij} - \partial_{t} \mathbf{A}_{i} - \sum_{j=1}^{N} (\mathbf{v}_{j} \cdot \nabla_{j}) \mathbf{A}_{i}, \qquad (3.3)$$

where $\mathbf{v}_j = \mathbf{p}_j^*/m_j$. The right side of the equation corresponds to the force that can be separated into three parts. The term j=i gives the self-"Lorentz force". $F_i^{\text{Lorentz}} =$

 $-\nabla_i A_{0,i} - \partial_t \mathbf{A}_i + \mathbf{v}_i \times (\nabla_i \times \mathbf{A}_i)$, where $-\nabla_i A_{0,i} - \partial_t \mathbf{A}_i = \mathbf{E}_i$ and $\nabla_i \times \mathbf{A}_i = \mathbf{B}_i$ can be interpreted as the "electric" and "magnetic" field, respectively. Then we obtain the familiar form $F_i^{\text{Lorentz}} = \mathbf{E}_i + \mathbf{v}_i \times \mathbf{B}_i$. This is the "self-force", which means particle i interacting with its own potentials A_i^{μ} . The term $j \neq i$ gives the mutual interaction force, $F_i^{\text{Mutual}} = \sum_{j \neq i} [\mathbf{v}_j \nabla_i \mathbf{A}_j - \nabla_i A_{0,j} - (\mathbf{v}_j \cdot \nabla_j) \mathbf{A}_i]$, which represents the force on particle i due to all other particles j through their interactions. $\mathbf{v}_j \nabla_i \mathbf{A}_j$ is the direct coupling of the current of particle j to the motion of particle i. It describes how the vector potential of i changes due to the presence of particle j. $-(\mathbf{v}_j \cdot \nabla_j) \mathbf{A}_i$ looks like a back-reaction term: it accounts for how the potential of i is influenced by the spatial derivative with respect to the source coordinate j. Physically, it enforces action–reaction consistency between the pair i and j. $-\nabla_i A_{0,j}$ represents the electric field force at i generated by particle j. Together, these terms represent the electromagnetic interaction between different particles mediated by the vector potential. The last one is the force induced by the potential V, $F_i^V = -\sum_{j \neq i} \nabla_i V_{ij}$.

4 Relativistic time evolution of two-body systems

4.1 Formal development of the time evolution equations with scalar and vector potentials

Now, let's examine the relativisite two-body case. First-class constraints are usually linked to mass shell conditions. We begin with the mass shell constraints of a two-particle system,

$$H_1 = p_{1,\mu} p_1^{\mu} - m_1^2,$$

$$H_2 = p_{2,\mu} p_2^{\mu} - m_2^2.$$
(4.1)

The vector interaction, A_{μ} , and the scalar interaction, Φ_i , can be introduced in a system of two interacting particles,

$$H_1 = p_{1,\mu}^* p_1^{*\mu} - m_1^2 + \Phi_1,$$

$$H_2 = p_{2,\mu}^* p_2^{*\mu} - m_2^2 + \Phi_2.$$
(4.2)

where $p_{i,\mu}^*$ is the mechanical momentum, which is related to the canonical momentum $p_{i,\mu}$ via, e.g. $p_{i,\mu}^* \equiv p_{i,\mu} - A_{i,\mu}$. The requirement that H_i is relativistic invariant implied that the potential Φ_i is a function of relativistic invariants only. Although the dimension of H_i is energy square, we call H_i Hamiltonian. The total Dirac Hamiltonian is $H = \lambda_1 H_1 + \lambda_2 H_2$. In order to make sure that H_1 and H_2 are conserved in the evolution, which means $\dot{H}_i = \{H_i, H\} \approx 0$, the H_i should satisfy the constraint,

$$\{H_1, H_2\} = 2p_1^{*\mu} \frac{\partial \Phi_2}{\partial q_1^{\mu}} - 2p_2^{*\mu} \frac{\partial \Phi_1}{\partial q_2^{\mu}} + \{\Phi_1, \Phi_2\} = 0. \tag{4.3}$$

The simplest way to satisfy the above equation is to take it as a relativistic counterpart of Newton's third law, which leads to an interaction-independent constraint. As said Φ_i

has to be relativistically invariant. One possibility to fulfill this demand is that Φ_i depends on q_T^2 .

$$\Phi_1 = \Phi_2 = \Phi(\sqrt{-q_T^2}),\tag{4.4}$$

where

$$q_T^2 \equiv q_T^{\mu} q_{T,\mu} = q^2 - \frac{(q_{\nu} P^{\nu})^2}{P^2} \tag{4.5}$$

and

$$q_T^{\mu} = \left(g^{\mu\nu} - \frac{P^{\mu}P^{\nu}}{P^2}\right)q_{\nu} = q^{\mu} - \frac{q_{\nu}P^{\nu}}{P^2}P^{\mu} \tag{4.6}$$

with $q^{\mu} = q_1^{\mu} - q_2^{\mu}$ and $P^{\mu} = p_1^{\mu} + p_2^{\mu}$. In the center-of-mass frame the transverse distance q_T^i represents the ordinary distance $q_1^i - q_2^i$ between the two particles and $q_T^0 = 0$.. With this choice we obtain for Eq. (4.3)

$$\{H_1, H_2\} = 4P^{\mu}q_{T,\mu}\frac{\partial\Phi(q_T)}{\partial q_T^2} = 0.$$
 (4.7)

so the constraint is fulfilled.

The equations of motion can be expressed as,

$$\frac{dq_i^{\mu}}{d\tau} = \{q_i^{\mu}, H\} = \lambda_1 \{q_i^{\mu}, H_1\} + \lambda_2 \{q_i^{\mu}, H_2\},
\frac{dp_i^{\mu}}{d\tau} = \{p_i^{\mu}, H\} = \lambda_1 \{p_i^{\mu}, H_1\} + \lambda_2 \{p_i^{\mu}, H_2\}.$$
(4.8)

 λ_1 and λ_2 are parameters, which can be fixed by introducing the second-class constraints. This will be discussed below. To obtain a world line of the two-body system, one needs still two constraints, $\chi_1(q_1, q_2, p_1, p_2) = 0$ and $\chi_2(q_1, q_2, p_1, p_2, \tau) = 0$. These two additional constraints reduce the 14-dimensional phase space to a 12-dimensional phase space with a parameter τ so effectively to a 13-dimensional phase space. The conservation of these constraints in τ gives,

$$\frac{d\chi_1}{d\tau} = \frac{\partial \chi_1}{\partial \tau} + \lambda_1 \{ \chi_1, H_1 \} + \lambda_2 \{ \chi_1, H_2 \} = 0,
\frac{d\chi_2}{d\tau} = \frac{\partial \chi_2}{\partial \tau} + \lambda_1 \{ \chi_2, H_1 \} + \lambda_2 \{ \chi_2, H_2 \} = 0.$$
(4.9)

This equation can be written in a matrix form,

$$\begin{pmatrix} \{\chi_1, H_1\} & \{\chi_1, H_2\} \\ \{\chi_2, H_1\} & \{\chi_2, H_2\} \end{pmatrix} \begin{pmatrix} \lambda_1 \\ \lambda_2 \end{pmatrix} = \begin{pmatrix} -\frac{\partial \chi_1}{\partial \tau} \\ -\frac{\partial \chi_2}{\partial \tau} \end{pmatrix}. \tag{4.10}$$

We can obtain the parameters λ_i by solving this eigen equation. If one defines,

$$S_{ij} \equiv \begin{pmatrix} \{\chi_1, H_1\} & \{\chi_1, H_2\} \\ \{\chi_2, H_1\} & \{\chi_2, H_2\} \end{pmatrix}$$

$$(4.11)$$

the inverse 2×2 matrix can be obtained analytically,

$$S_{ij}^{-1} = \frac{1}{\{\chi_1, H_1\}\{\chi_2, H_2\} - \{\chi_1, H_2\}\{\chi_2, H_1\}} \begin{pmatrix} \{\chi_2, H_2\} - \{\chi_1, H_2\} \\ -\{\chi_2, H_1\} & \{\chi_1, H_1\} \end{pmatrix}. \tag{4.12}$$

and the λ_i can be expressed as,

$$\lambda_i = -\sum_{j=1}^2 S_{ij}^{-1} \frac{d\chi_j}{d\tau}.$$
 (4.13)

So for given time constraints, χ_i , the EoMs, Eq. (4.8), are determined once λ_1, λ_2 are calculated. It is important to realize that different time constraints may lead to different EoMs.

For the second-class constraints of the two particles, we first assume:

$$\chi_1 = \frac{1}{2}(q_1^{\mu} - q_2^{\mu})U_{\mu} = 0, \quad \chi_2 = \frac{1}{2}(q_1^{\mu} + q_2^{\mu})U_{\mu} - \tau = 0,$$
(4.14)

where $U_{\mu} = P_{\mu}/\sqrt{P^2}$ is the four velocity of the center of mass system. We can see immediately that the constraint χ_1 is time independent because $\{\chi_1, G\} = 0$. The second constraint defines a uniform evolution time τ , which is, in the center-of-mass frame, equal to $\tau = (t_1^{com} + t_2^{com})/2$. The evolution is calculated as a function of τ but we can reconstruct the times t_1 and t_2 via the time constraints,

$$t_1 = \frac{1}{U^0} (\tau + x_1 U_x + y_1 U_y + z_1 U_z),$$

$$t_2 = \frac{1}{U^0} (\tau + x_2 U_x + y_2 U_y + z_2 U_z).$$
(4.15)

Thus, the times of the two particles, t_1 and t_2 , are not free parameters, but connected by the constraints and are functions to the coordinates and momenta of the two particles. If the total momentum is zero, then $t_1 = t_2 = \tau$. In this case, the zero (time) component of the coordinate space 4-vector coincides with the the system time τ .

The Poisson brackets of the time-constraints and the Hamiltonian can be expressed as,

$$\begin{aligned}
\{\chi_{1}, H_{1}\} &= U_{\mu} p_{1}^{*\nu} \left(\frac{\partial p_{1,\nu}^{*}}{\partial p_{1,\mu}} - \frac{\partial p_{1,\nu}^{*}}{\partial p_{2,\mu}} \right) + \frac{U_{\mu}}{2} \left(\frac{\partial \Phi_{1}}{\partial p_{1,\mu}} - \frac{\partial \Phi_{1}}{\partial p_{2,\mu}} \right), \\
\{\chi_{1}, H_{2}\} &= U_{\mu} p_{2}^{*\nu} \left(\frac{\partial p_{2,\nu}^{*}}{\partial p_{1,\mu}} - \frac{\partial p_{2,\nu}^{*}}{\partial p_{2,\mu}} \right) + \frac{U_{\mu}}{2} \left(\frac{\partial \Phi_{2}}{\partial p_{1,\mu}} - \frac{\partial \Phi_{2}}{\partial p_{2,\mu}} \right), \\
\{\chi_{2}, H_{1}\} &= U_{\mu} p_{1}^{*\nu} \left(\frac{\partial p_{1,\nu}^{*}}{\partial p_{1,\mu}} + \frac{\partial p_{1,\nu}^{*}}{\partial p_{2,\mu}} \right) + \frac{U_{\mu}}{2} \left(\frac{\partial \Phi_{1}}{\partial p_{1,\mu}} + \frac{\partial \Phi_{1}}{\partial p_{2,\mu}} \right), \\
\{\chi_{2}, H_{2}\} &= U_{\mu} p_{2}^{*\nu} \left(\frac{\partial p_{2,\nu}^{*}}{\partial p_{1,\mu}} + \frac{\partial p_{2,\nu}^{*}}{\partial p_{2,\mu}} \right) + \frac{U_{\mu}}{2} \left(\frac{\partial \Phi_{2}}{\partial p_{1,\mu}} + \frac{\partial \Phi_{2}}{\partial p_{2,\mu}} \right).
\end{aligned} \tag{4.16}$$

If the scalar potential, Φ_i , does not depend explicitly on the particle's momentum, then the derivative of Φ_i with respect to momentum gives

$$\frac{\partial \Phi_i}{\partial p_{i,\mu}} = \frac{\partial \Phi_i}{\partial q_T^2} \frac{\partial q_T^2}{\partial p_{i,\mu}},\tag{4.17}$$

where

$$\frac{\partial q_T^2}{\partial p_{i,\mu}} = -2 \frac{(q_1^{\mu} - q_2^{\mu})P_{\mu}}{P^2} q_{T,\mu} = 0, \tag{4.18}$$

due to the constraint χ_1 . Therefore, the momentum derivative of the Φ_i disappears when second-class constraints like Eq. (4.14) are chosen.

With these preparations, we can calculate the λ_i (4.13) explicitly

$$\lambda_{1} = \frac{U_{\mu}p_{2}^{*\nu} \left(\frac{\partial p_{2,\nu}^{*}}{\partial p_{1,\mu}} - \frac{\partial p_{2,\nu}^{*}}{\partial p_{2,\mu}}\right)}{2\left(U_{\mu}p_{1}^{*\nu}\frac{\partial p_{1,\nu}^{*}}{\partial p_{2,\mu}}\right) * \left(U_{\mu}p_{2}^{*\nu}\frac{\partial p_{2,\nu}^{*}}{\partial p_{1,\mu}}\right) - 2\left(U_{\mu}p_{1}^{*\nu}\frac{\partial p_{1,\nu}^{*}}{\partial p_{1,\mu}}\right) * \left(U_{\mu}p_{2}^{*\nu}\frac{\partial p_{2,\nu}^{*}}{\partial p_{2,\mu}}\right)},
\lambda_{2} = \frac{U_{\mu}p_{1}^{*\nu} \left(\frac{\partial p_{1,\nu}^{*}}{\partial p_{2,\mu}} - \frac{\partial p_{1,\nu}^{*}}{\partial p_{1,\mu}}\right)}{2\left(U_{\mu}p_{1}^{*\nu}\frac{\partial p_{1,\nu}^{*}}{\partial p_{2,\mu}}\right) * \left(U_{\mu}p_{2}^{*\nu}\frac{\partial p_{2,\nu}^{*}}{\partial p_{1,\mu}}\right) - 2\left(U_{\mu}p_{1}^{*\nu}\frac{\partial p_{1,\nu}^{*}}{\partial p_{1,\mu}}\right) * \left(U_{\mu}p_{2}^{*\nu}\frac{\partial p_{2,\nu}^{*}}{\partial p_{2,\mu}}\right)}.$$
(4.19)

Moreover, we find for the Poisson brackets of the coordinates q_i and momenta p_i with the Hamiltonian

$$\{q_i^{\mu}, H_i\} = 2p_i^{*\nu} \frac{\partial p_{i,\nu}^*}{\partial p_{i,\mu}} + \frac{\partial \Phi_i}{\partial p_{i,\mu}},$$

$$\{q_i^{\mu}, H_j\} = 2p_j^{*\nu} \frac{\partial p_{j,\nu}^*}{\partial p_{i,\mu}} + \frac{\partial \Phi_j}{\partial p_{i,\mu}},$$

$$\{p_i^{\mu}, H_i\} = -2p_i^{*\nu} \frac{\partial p_{i,\nu}^*}{\partial q_{i,\mu}} - \frac{\partial \Phi_i}{\partial q_{i,\mu}},$$

$$\{p_i^{\mu}, H_j\} = -2p_j^{*\nu} \frac{\partial p_{j,\nu}^*}{\partial q_{i,\mu}} - \frac{\partial \Phi_j}{\partial q_{i,\mu}}.$$

$$(4.20)$$

Then, the equations of motion (EoMs) for the interacting two-body system (4.8) can be written as,

$$\frac{dq_i^{\mu}}{d\tau} = \sum_{k=1}^{2} \lambda_k \left(2p_k^{*\nu} \frac{\partial p_{k,\nu}^*}{\partial p_{i,\mu}} \right),$$

$$\frac{dp_i^{\mu}}{d\tau} = -\sum_{k=1}^{2} \lambda_k \left(2p_k^{*\nu} \frac{\partial p_{k,\nu}^*}{\partial q_{i,\mu}} + \frac{\partial \Phi_k}{\partial q_{i,\mu}} \right).$$
(4.21)

4.2 Relation to the RQMD, UrQMD, and JAM

Now, let us examine the connection between the equations of motion derived above and those employed in transport models such as RQMD, UrQMD, and JAM.

For a system with a scalar potential only, the λ_i is simplified,

$$\lambda_1 = (2p_1^{\mu}U_{\mu})^{-1},$$

$$\lambda_2 = (2p_2^{\mu}U_{\mu})^{-1},$$
(4.22)

and the above EoMs read as,

$$\frac{dq_i^{\mu}}{d\tau} = \frac{p_i^{\mu}}{p_i^{\mu}U_{\mu}},$$

$$\frac{dp_i^{\mu}}{d\tau} = -\sum_{k=1}^{2} \frac{1}{2p_k^{\mu}U_{\mu}} \frac{\partial \Phi_k}{\partial q_{i,\mu}},$$
(4.23)

These are exactly the EoMs used in RQMD [28–30] and UrQMD [35]. RQMD [28] applied a scalar potential of the same functional form as used in non-relativistic QMD calculations, in which the non-relativistic density is replaced by the scalar density. In practice UrQMD calculations use non-relativistic potentials [53].

In the JAM approach [32–34] different time constraints have been employed:

$$\chi_1 = (q_1^{\mu} - q_2^{\mu})U_{\mu} = 0, \quad \chi_2 = q_2^{\mu}U_{\mu} - \tau = 0.$$
(4.24)

The equations of motion can be obtained using similar procedures as before

$$\frac{dq_i^{\mu}}{d\tau} = \lambda_i 2p_i^{*\mu} - g^{\mu\sigma} \sum_{k=1}^2 \lambda_k \left[2p_k^{*\nu} \frac{\partial V_{k,\nu}}{\partial p_i^{\sigma}} + \frac{\partial m_k^{*2}}{\partial p_i^{\sigma}} \right],$$

$$\frac{dp_i^{\mu}}{d\tau} = g^{\mu\sigma} \sum_{k=1}^2 \lambda_k \left[2p_k^{*\nu} \frac{\partial V_{k,\nu}}{\partial q_i^{\sigma}} + \frac{\partial m_k^{*2}}{\partial q_i^{\sigma}} \right].$$
(4.25)

The notation of $p_i^* = p_i - V_i$ and $m_i^* = m_i - S_i$ are used. V_i and S_i denote the vector and scalar potential in their paper, respectively. The scalar potential modifies the particle's mass. There are two common ways for its implementation. The first is to redefine the mass directly as $m^* \equiv m - S$, leading to the constraint $H_i = p_{1,\mu}^* p_1^{*\mu} - (m_i - S_i)^2$. The second approach is to add the scalar part explicitly in the Hamiltonian, $H_i = p_{1,\mu}^* p_1^{*\mu} - m_i^2 + 2m_i S$. Both formulations yield the same non-relativistic limit if $|S_i| \ll m_i$, $|A_i^{\mu}| \ll m_i$, and $|\mathbf{p}| \ll m_i$. The second formulation give the non-relativistic limit also for arbitrary $|S_i|$ and therefore we apply it here.

If one neglects the momentum-dependent derivatives of the vector potential in the expression of λ_i (Eq. (4.19)) $(\frac{\partial p_{2,\nu}^*}{\partial p_{1,\mu}} = 0, \frac{\partial p_{2,\nu}^*}{\partial p_{2,\mu}} = 1)$, one arrives at

$$\lambda_1 = \frac{1}{2p_1^{*\mu}U_{\mu}},$$

$$\lambda_2 = \frac{1}{2p_2^{*\mu}U_{\mu}}.$$
(4.26)

If one further assumes $2p_i^{*\mu}U_{\mu}=2p_i^{*0}$, what is fulfilled in the CoM frame but not in other reference frames, the expressions of λ_i simplify further and one obtains the approximate EoM

$$\frac{dq_{i}^{\mu}}{d\tau} = \frac{p_{i}^{*\mu}}{p_{i}^{*0}} - g^{\mu\sigma} \sum_{k=1}^{2} \left[\frac{p_{k}^{*\nu}}{p_{k}^{*0}} \frac{\partial V_{k,\nu}}{\partial p_{i}^{\sigma}} + \frac{m_{k}^{*}}{p_{k}^{*0}} \frac{\partial m_{k}^{*}}{\partial p_{i}^{\sigma}} \right],$$

$$\frac{dp_{i}^{\mu}}{d\tau} = g^{\mu\sigma} \sum_{k=1}^{2} \left[\frac{p_{i}^{*\nu}}{p_{i}^{*0}} \frac{\partial V_{k,\nu}}{\partial q_{i}^{\sigma}} + \frac{m_{k}^{*}}{p_{k}^{*0}} \frac{\partial m_{k}^{*}}{\partial q_{i}^{\sigma}} \right],$$
(4.27)

and for the 3-components, if with $g^{\mu\nu}=(+,-,-,-)$:

$$\frac{d\mathbf{q}_{i}}{d\tau} = \frac{\mathbf{p}_{i}^{*}}{p_{i}^{*0}} + \sum_{k=1}^{2} \left[\frac{\mathbf{p}_{k}^{*}}{p_{k}^{*0}} \frac{\partial V_{k}}{\partial \mathbf{p}_{i}} + \frac{m_{k}^{*}}{p_{k}^{*0}} \frac{\partial m_{k}^{*}}{\partial \mathbf{p}_{i}} \right],$$

$$\frac{d\mathbf{p}_{i}}{d\tau} = -\sum_{k=1}^{2} \left[\frac{\mathbf{p}_{i}^{*}}{p_{i}^{*0}} \frac{\partial V_{k,v}}{\partial \mathbf{q}_{i}} + \frac{m_{k}^{*}}{p_{k}^{*0}} \frac{\partial m_{k}^{*}}{\partial \mathbf{q}_{i}} \right].$$

$$(4.28)$$

These equations are the basis for he numerical calculations in JAM [32–34]. For actual calculations the scalar and vector densities are converted into σ and ω mean fields, which are subsequently used in these EoMs.

4.3 The non-relativistic limit

After having defined the EoMs one can numerically calculate the trajectories of the two particles. We will consider here only the scalar potential (4.23) (the vector potential we will discuss in subsection 4.5) to check the non-relativistic limit. In this test, we use $V(q_T) = \frac{c}{2}m\omega^2|q_T^2|$, which reduces in the center of mass to the harmonic oscillator potential $V(r) = \frac{c}{2}m\omega^2r^2$. For the following numerical calculation, we set $m_1 = m_2 = m = 1$ GeV and set the frequency ω to be equal to 0.05 GeV. In the relativistic case, $\Phi_1 = \Phi_2 = 2\mu V(q_T)$ with the reduced mass $\mu = m/2$. The parameter $c = \pm 1$ corresponds to an attractive or repulsive potential, respectively.

We use two initial conditions for the two particles:

I.
$$\mathbf{x}_1 = (-0.5, 0, 0)$$
 fm, $\mathbf{x}_2 = (0.5, 0, 0)$ fm, $\mathbf{p}_1 = (5, 0, 0)$ GeV, $\mathbf{p}_2 = (1, 0, 0)$ GeV;

II.
$$\mathbf{x}_1 = (-1.0, 0, 0)$$
 fm, $\mathbf{x}_2 = (1.0, 0, 0)$ fm, $\mathbf{p}_1 = (5, 0, 0)$ GeV, $\mathbf{p}_2 = (-5, 0, 0)$ GeV.

The first initial condition gives a total momentum is $P_{\text{tot}} = 6 \text{ GeV}$, while for the second one is $P_{\text{tot}} = 0$.

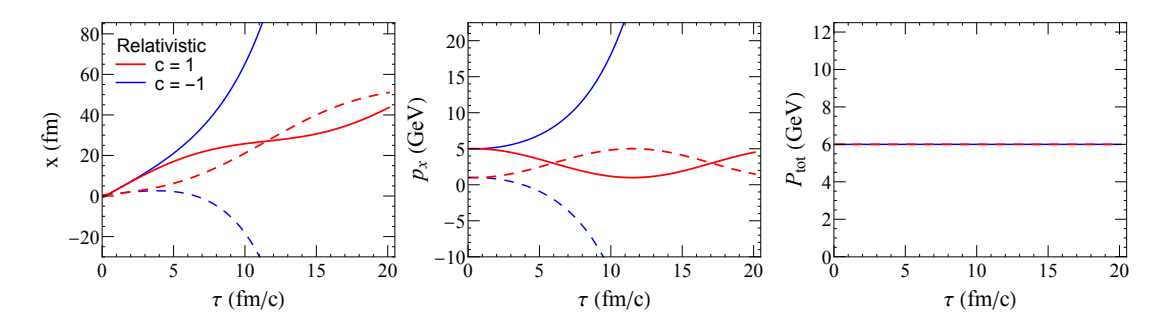


Figure 2. The coordinates and momenta of particles 1 (solid lines) and 2 (dashed lines) as a function of computational time τ in relativistic evolutions. The red and blue lines represent an attractive (c=1) and a repulsive interaction (c=-1), respectively. The initial condition I is taken.

We start with the initial condition I and evolve the two-particle system with either a repulsive or an attractive potential. The results are shown in Fig. 2. For the attractive

potential (red curves), the two particles exhibit a spiral motion toward each other, while for the repulsive potential (blue curves), they move apart, as expected. Throughout the evolution, the total momentum of the system is conserved, as seen on the left plot. Since the initial momenta and positions in the y- and z-directions are set to zero $p_y = p_z = 0 = y = z$, these components remain zero during the entire evolution.

We can see that the solution of the relativistic equations of motion (4.21) approaches that of the non-relativistic ones (3.2) in the non-relativistic limit, obtained for $m \to \infty$. We now verify this limit numerically using the harmonic oscillator potential and set the particle mass to m = 20 GeV, which is large enough to expect non relativistic kinematics. The results are shown in Fig. 3. In this case, the computational time $\tau \approx t_1 \approx t_2$ from Eq. (4.15), due to $U^{\mu} \approx (1,0,0,0)$. Consequently, the trajectories can be plotted together for direct comparison. As expected, the trajectories from both the relativistic and non-relativistic calculations are identical in this limit.

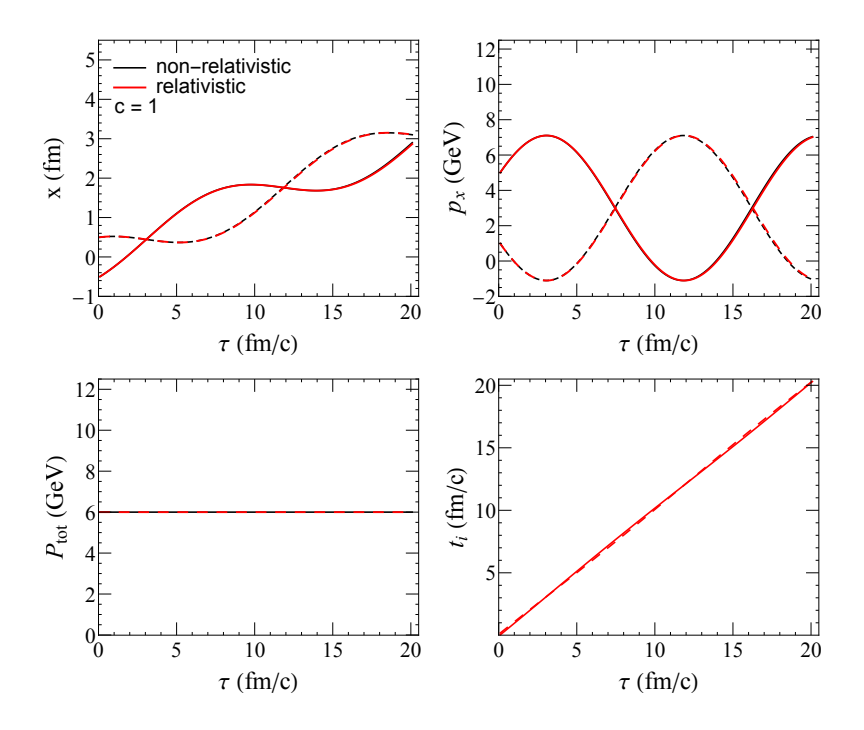


Figure 3. The coordinates and momenta of particle 1 (solid lines) and 2 (dashed lines). The black and red line represent the non-relativistic and relativistic evolution with a mass m=20 GeV, respectively. Here we take c=1, which means an attractive interaction between two particles. The initial condition I is taken.

It is worth emphasizing that even if the total momentum of the system is zero, relativistic effects can still manifest themselves in the dynamics. To illustrate this, we performed a simulation using initial condition II, as shown in Fig. 4. In this scenario, $\tau = t_1 = t_2$ holds exactly because $U^{\mu} = (1,0,0,0)$. This allows for a direct comparison between the relativistic and non-relativistic trajectories within the same figure. The key difference in the equations of motion is that, in the non-relativistic case, the velocity term takes the form p/m, whereas in the relativistic case it becomes p/E. The results clearly show that

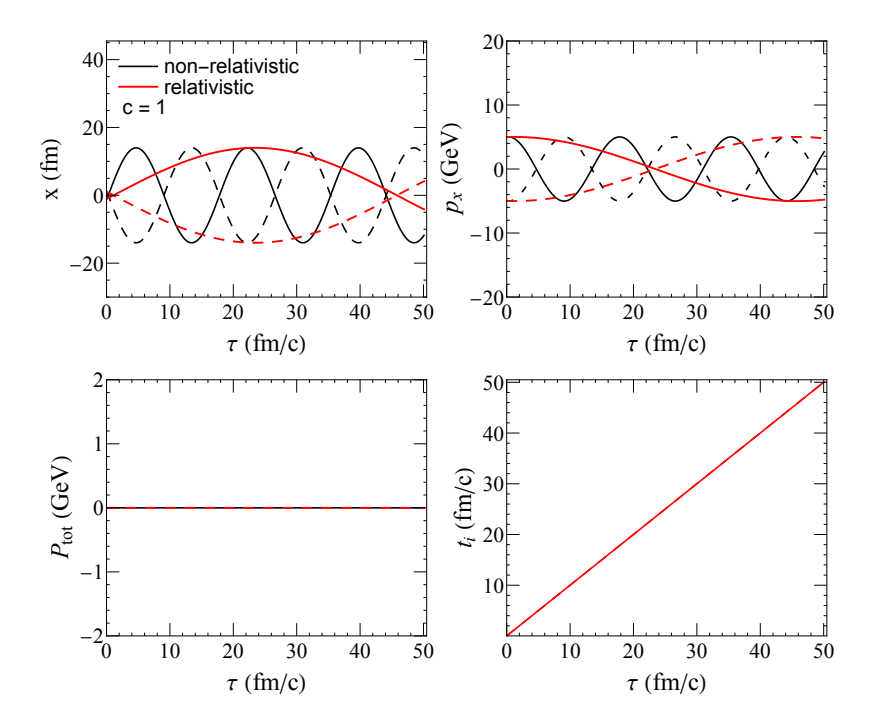


Figure 4. The coordinates and momentum of particle 1 (solid lines) and 2 (dashed lines). The black and red line represent the non-relativistic and relativistic evolution, respectively. Here we take c=1, which means an attractive interaction between the two particles. The initial condition II is chosen with $P_{\rm tot}=0$.

the "frequency" of the spiral motion is larger in the non-relativistic case compared to the relativistic one. This highlights that relativistic corrections can significantly modify the dynamical behavior of the system, even when the total momentum vanishes.

4.4 Different choices of time constraints

We examine now the influence of the time constraints. In principle, we can choose any time constraint as long as it satisfies the world line invariance and Poincaré transformation, discussed before. Two of them (4.14) and (4.24) we discussed already in section 4.3. For a scalar potential only, both yield the equations of motion

$$\frac{dq_i^{\mu}}{d\tau} = \frac{p_i^{\mu}}{p_i^{\mu}U_{\mu}},$$

$$\frac{dp_i^{\mu}}{d\tau} = -\sum_{k=1}^{2} \frac{1}{2p_k^{\mu}U_{\mu}} \frac{\partial \Phi_k}{\partial q_{i,\mu}}.$$
(4.29)

as already discussed. One may also obtain different EoMs. This is shown by using other time-constraints, which also satisfies the world line invariance and Poincaré transformation,

$$\chi_1 = \frac{1}{2}(q_1^{\mu} - q_2^{\mu})U_{\mu} = 0, \quad \chi_2 = \frac{1}{2}q_1^{\mu}U_{\mu} - \tau = 0.$$
(4.30)

The related λ_i can be calculated as

$$\lambda_1 = (p_1^{\mu} U_{\mu})^{-1},$$

$$\lambda_2 = (p_2^{\mu} U_{\mu})^{-1}.$$
(4.31)

Then, the equations of motion become,

$$\frac{dq_i^{\mu}}{d\tau} = \frac{2p_i^{\mu}}{p_i^{\mu}U_{\mu}},$$

$$\frac{dp_i^{\mu}}{d\tau} = -\sum_{k=1}^{2} \frac{1}{p_k^{\mu}U_{\mu}} \frac{\partial \Phi_k}{\partial q_{i,\mu}}.$$
(4.32)

Also in this case, the times t_1 and t_2 can be calculated via the time constraints,

$$t_1 = \frac{1}{U^0} (2\tau + x_1 U_x + y_1 U_y + z_1 U_z),$$

$$t_2 = t_1 - \frac{1}{U^0} [(x_1 - x_2) U_x + (y_1 - y_2) U_y + (z_1 - z_2) U_z].$$
(4.33)

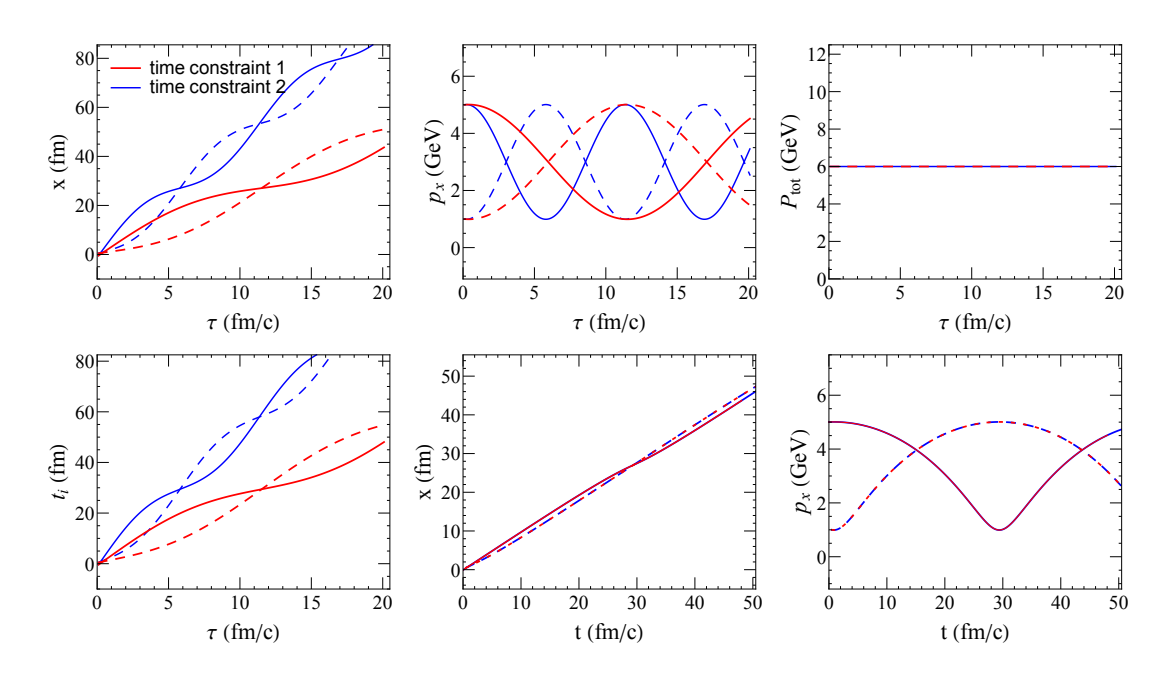


Figure 5. The coordinates and momenta of particles 1 (solid lines) and 2 (dashed lines). The red and blue lines represent the results for two different time constraints, Eq. (4.14), and Eq. (4.30), respectively. Here we take an attractive interaction between the two particles (c = 1). The initial condition I is chosen.

In this case, although the equations of motion (EoM) cannot be directly reduced to the non-relativistic form, the particle trajectories are identical. This is ensured by the World line invariance condition. The results obtained, using the previous time constraint, Eq. (4.14), and the new time constraint, Eq. (4.30), are shown in Fig. 5. As we can see it is

really not visible you have to present the curves in a different form, the trajectories plotted as a function of the computational time τ appear different for the two time constraints. However, when we take into account the relation between the computational time τ and the times t_i of the particles, we can calculate the trajectories $\mathbf{x}_i(t_i)$. After performing this transformation, we find that the physical particle trajectories are indeed identical under both time constraints, as shown in the bottom right panel. This confirms that, despite differences in parametrization with respect to τ , the actual space-time evolution of the system remains unchanged, consistent with the requirement of world line invariance, as discussed in section 2.

4.5 Numerical study of a two-nucleon system with scalar and vector interactions

We derive the relativistic equations of motion for the purpose to study the equation of state (EoS) of strongly interacting matter, the energy as a function of baryon density and temperature. To obtain this quantity is one of the primary goals of relativistic heavy ion collisions. Its knowledge is of importance for other fields of physics like that of neutron stars and gravitational waves. To explore the equation of state, experimental results of heavy-ion collisions are compared with that of transport approaches. In these transport approaches usually a so called Schrödinger equivalent potential (SEP) is used [38]. Sometimes the momentum dependence of this potential is even completely neglected. The SEP arises from the non-relativistic reduction of the Dirac equation with relativistic scalar and vector mean fields. It provides an effective central potential that can be constrained, for densities below nuclear saturation, through analyses of elastic proton-nucleus scattering data. However, this approximation scheme breaks down at beam energies in the GeV-per-nucleon regime. The reason is that the reduction to a single SEP conceals the very different dynamical roles of scalar and vector fields: the scalar potential modifies the effective mass of the particle, while the vector potential shifts the particle 4- momentum and acts differently in the equations of motion. At low energies, where the difference between scalar density and vector density (the zero component of the baryon 4-current) is small, the simplification in the SEP to identify both with the scalar density is justified, as it has been done in static Skyrme-type potentials, which are frequently used in low energy calculations. At higher beam energies this approximation becomes inadequate, because the distinct roles of scalar and vector fields become crucial. In a fully relativistic EoM the scalar and vector fields enter the EoMs differently, as shown in Eq. (4.2) and (4.21), and will influence the time evolution of particle trajectories in qualitatively different ways.

When proceeding to the study of covariant time-evolution equations for a two-body system, interacting via scalar and vector potentials, we adopt forms of these potentials that are particularly suited for future investigations of the EoS.

$$A_i^{\mu} = \sum_{j \neq i}^{N} p_j^{*\mu} \rho_{ij}(q_T), \quad S_i = \sum_{j \neq i}^{N} m_i \rho_{ij}(q_T),$$
 (4.34)

is on the one side of a form, which can be used to study an interacting system of nucleons

[54–56] and offers on the other side the possibility to study the different influence of scalar and vector potentials on nuclear trajectories.

For a two-body system we employ

$$A_1^{\mu} = p_2^{*\mu} \rho_{12}(q_T),$$

$$A_2^{\mu} = p_1^{*\mu} \rho_{12}(q_T),$$

$$\Phi_1 = \Phi_2 = 2\mu S = 2\mu m \rho_{12}(q_T),$$
(4.35)

where $\mu = m_1 m_2/(m_1 + m_2)$ is the reduced mass. $p_i^{*\mu} = p_i^{\mu} - A_i^{\mu}$ is the mechanical momentum. In the numerical calculation, we take, of not otherwise stated, $m_1 = m_2 = m = 1$ GeV. The definition of the density ρ_{12} is [57]

$$\rho_{12}(q_T) = \frac{\kappa}{(2\pi L)^{3/2}} \exp(q_T^2/(2L)), \tag{4.36}$$

where the Gaussian width is taken as $L = 1.5 \text{ fm}^2$. κ is a parameter with the dimension of fm³, which is introduced to ensure that ρ is dimensionless.

From the above definition, we can show that the A_i^{μ} can be expressed as

$$A_1^{\mu} = \frac{p_2^{\mu} \rho_{12} - p_1^{\mu} \rho_{12}^2}{1 - \rho_{12}^2},$$

$$A_2^{\mu} = \frac{p_1^{\mu} \rho_{12} - p_2^{\mu} \rho_{12}^2}{1 - \rho_{12}^2},$$
(4.37)

This allows to calculate the derivative terms,

$$\begin{split} \frac{\partial p_{1,\nu}^*}{\partial p_{1,\mu}} &= \frac{1}{1 - \rho_{12}^2} \delta_{\nu}^{\mu}, \\ \frac{\partial p_{1,\nu}^*}{\partial p_{2,\mu}} &= \frac{-\rho_{12}}{1 - \rho_{12}^2} \delta_{\nu}^{\mu}, \\ \frac{\partial p_{2,\nu}^*}{\partial p_{1,\mu}} &= \frac{-\rho_{12}}{1 - \rho_{12}^2} \delta_{\nu}^{\mu}, \\ \frac{\partial p_{2,\nu}^*}{\partial p_{2,\mu}} &= \frac{1}{1 - \rho_{12}^2} \delta_{\nu}^{\mu}, \\ \frac{\partial \Phi}{\partial p_{i,\mu}} &= 0, \end{split}$$
(4.38)

and,

$$\frac{\partial p_{1,\nu}^*}{\partial q_{i,\mu}} = \frac{p_{2,\nu} - 2p_{1,\nu}\rho_{12} + p_{2,\nu}\rho_{12}^2}{(1 - \rho_{12}^2)^2} \frac{\partial \rho_{12}}{\partial q_{i,\mu}}, \quad i = 1, 2$$

$$\frac{\partial p_{2,\nu}^*}{\partial q_{i,\mu}} = \frac{p_{1,\nu} - 2p_{2,\nu}\rho_{12} + p_{1,\nu}\rho_{12}^2}{(1 - \rho_{12}^2)^2} \frac{\partial \rho_{12}}{\partial q_{i,\mu}}, \quad i = 1, 2$$

$$\frac{\partial \Phi}{\partial q_{i,\mu}} = 2\mu \frac{\partial \rho_{12}}{\partial q_{i,\mu}}, \quad i = 1, 2.$$
(4.39)

Following the similar procedure as shown at the beginning of Sec. 4, we find

$$\lambda_{1} = \frac{(1+\rho_{12})^{2}(1-\rho_{12})}{2(p_{1}^{\mu}-p_{2}^{\mu}\rho_{12})U_{\mu}},$$

$$\lambda_{2} = \frac{(1+\rho_{12})^{2}(1-\rho_{12})}{2(p_{2}^{\mu}-p_{1}^{\mu}\rho_{12})U_{\mu}}.$$
(4.40)

Finally, we obtain the explicit form of the EoMs from Eq. (4.21).

$$\frac{dq_{1}^{\mu}}{d\tau} = \frac{p_{1}^{\mu} - p_{2}^{\mu}\rho_{12}}{(p_{1}^{\mu} - p_{2}^{\mu}\rho_{12})U_{\mu}} \frac{1}{1 - \rho_{12}} - \frac{p_{2}^{\mu} - p_{1}^{\mu}\rho_{12}}{(p_{2}^{\mu} - p_{1}^{\mu}\rho_{12})U_{\mu}} \frac{\rho_{12}}{1 - \rho_{12}},$$

$$\frac{dq_{2}^{\mu}}{d\tau} = \frac{p_{1}^{\mu} - p_{2}^{\mu}\rho_{12}}{(p_{1}^{\mu} - p_{2}^{\mu}\rho_{12})U_{\mu}} \frac{-\rho_{12}}{1 - \rho_{12}} + \frac{p_{2}^{\mu} - p_{1}^{\mu}\rho_{12}}{(p_{2}^{\mu} - p_{1}^{\mu}\rho_{12})U_{\mu}} \frac{1}{1 - \rho_{12}},$$

$$\frac{dp_{1}^{\mu}}{d\tau} = \left[\frac{(p_{1}^{\nu} - p_{2}^{\nu}\rho_{12})(p_{2,\nu} - 2p_{1,\nu}\rho_{12} + p_{2,\nu}\rho_{12}^{2})}{(p_{1}^{\mu} - p_{2}^{\mu}\rho_{12})U_{\mu}} \frac{1}{(1 + \rho_{12})(1 - \rho_{12})^{2}} \right] \frac{\partial \rho_{12}}{\partial q_{1,\mu}}$$

$$+ \left[\frac{(p_{2}^{\nu} - p_{1}^{\nu}\rho_{12})(p_{1,\nu} - 2p_{2,\nu}\rho_{12} + p_{1,\nu}\rho_{12}^{2})}{(p_{2}^{\mu} - p_{1}^{\mu}\rho_{12})U_{\mu}} \frac{1}{(1 + \rho_{12})(1 - \rho_{12})^{2}} \right] \frac{\partial \rho_{12}}{\partial q_{1,\mu}}$$

$$- \frac{(1 + \rho_{12})^{2}(1 - \rho_{12})\mu}{(p_{1}^{\mu} - p_{2}^{\mu}\rho_{12})U_{\mu}} \frac{\partial \rho_{12}}{\partial q_{1,\mu}} - \frac{(1 + \rho_{12})^{2}(1 - \rho_{12})\mu}{(p_{2}^{\mu} - p_{1}^{\mu}\rho_{12})U_{\mu}} \frac{\partial \rho_{12}}{\partial q_{1,\mu}},$$

$$\frac{dp_{2}^{\mu}}{d\tau} = \left[\frac{(p_{1}^{\nu} - p_{2}^{\nu}\rho_{12})(p_{2,\nu} - 2p_{1,\nu}\rho_{12} + p_{2,\nu}\rho_{12}^{2})}{(p_{1}^{\mu} - p_{2}^{\mu}\rho_{12})U_{\mu}} \frac{1}{(1 + \rho_{12})(1 - \rho_{12})^{2}} \right] \frac{\partial \rho_{12}}{\partial q_{2,\mu}}$$

$$+ \left[\frac{(p_{2}^{\nu} - p_{1}^{\nu}\rho_{12})(p_{1,\nu} - 2p_{2,\nu}\rho_{12} + p_{1,\nu}\rho_{12}^{2})}{(p_{2}^{\mu} - p_{1}^{\mu}\rho_{12})U_{\mu}} \frac{1}{(1 + \rho_{12})(1 - \rho_{12})^{2}} \right] \frac{\partial \rho_{12}}{\partial q_{2,\mu}}$$

$$- \frac{(1 + \rho_{12})^{2}(1 - \rho_{12})\mu}{(p_{1}^{\mu} - p_{2}^{\mu}\rho_{12})U_{\mu}} \frac{\partial \rho_{12}}{\partial q_{2,\mu}} - \frac{(1 + \rho_{12})^{2}(1 - \rho_{12})\mu}{(p_{2}^{\mu} - p_{1}^{\mu}\rho_{12})U_{\mu}} \frac{\partial \rho_{12}}{\partial q_{2,\mu}}$$

$$- \frac{(1 + \rho_{12})^{2}(1 - \rho_{12})\mu}{(p_{1}^{\mu} - p_{2}^{\mu}\rho_{12})U_{\mu}} \frac{\partial \rho_{12}}{\partial q_{2,\mu}} - \frac{(1 + \rho_{12})^{2}(1 - \rho_{12})\mu}{(p_{2}^{\mu} - p_{1}^{\mu}\rho_{12})U_{\mu}} \frac{\partial \rho_{12}}{\partial q_{2,\mu}}.$$

$$(4.41)$$

The non-relativisitic EoMs of the two-body system (Eq. (3.2)) can be written as,

$$\frac{d\mathbf{q}_{1}}{dt} = \frac{\mathbf{p}_{1} - 2\mathbf{p}_{2}\rho_{12} + \mathbf{p}_{1}\rho_{12}^{2}}{m(1 - \rho_{12}^{2})^{2}} + \frac{\mathbf{p}_{1}\rho_{12}}{m(1 + \rho_{12})},$$

$$\frac{d\mathbf{q}_{2}}{dt} = \frac{\mathbf{p}_{2} - 2\mathbf{p}_{1}\rho_{12} + \mathbf{p}_{2}\rho_{12}^{2}}{m(1 - \rho_{12}^{2})^{2}} + \frac{\mathbf{p}_{2}\rho_{12}}{m(1 + \rho_{12})},$$

$$\frac{d\mathbf{p}_{1}}{dt} = \left[\frac{2\mathbf{p}_{1} \cdot \mathbf{p}_{2} - 3(\mathbf{p}_{1}^{2} + \mathbf{p}_{2}^{2})\rho_{12} + 6\mathbf{p}_{1} \cdot \mathbf{p}_{2}\rho_{12}^{2} - (\mathbf{p}_{1}^{2} + \mathbf{p}_{2}^{2})\rho_{12}^{3}}{m(1 - \rho_{12}^{2})^{3}} - \frac{E_{1} + E_{2}}{(1 + \rho_{12})^{2}} \right] \frac{\partial \rho_{12}}{\partial \mathbf{q}_{1}} - \frac{\partial V}{\partial \mathbf{q}_{1}},$$

$$\frac{d\mathbf{p}_{2}}{dt} = \left[\frac{2\mathbf{p}_{1} \cdot \mathbf{p}_{2} - 3(\mathbf{p}_{1}^{2} + \mathbf{p}_{2}^{2})\rho_{12} + 6\mathbf{p}_{1} \cdot \mathbf{p}_{2}\rho_{12}^{2} - (\mathbf{p}_{1}^{2} + \mathbf{p}_{2}^{2})\rho_{12}^{3}}{m(1 - \rho_{12}^{2})^{3}} - \frac{E_{1} + E_{2}}{(1 + \rho_{12})^{2}} \right] \frac{\partial \rho_{12}}{\partial \mathbf{q}_{2}} - \frac{\partial V}{\partial \mathbf{q}_{2}},$$

where $E_i = m + \frac{p_i^2}{2m}$.

4.5.1 The influence of the vector and scalar potentials

To see the influence of the vector and scalar potential, we solve numerically the equations of motion for a two-body system with two initial conditions:

III.
$$\mathbf{x}_1 = (0, -1, -1)$$
 fm, $\mathbf{x}_2 = (0, 1, 1)$ fm, $\mathbf{p}_1 = (0, 0, 0)$ GeV, $\mathbf{p}_2 = (0, 0, 0)$ GeV;
IV. $\mathbf{x}_1 = (0, -1, -20)$ fm, $\mathbf{x}_2 = (0, 1, 20)$ fm, $\mathbf{p}_1 = (1, 0, 0)$ GeV, $\mathbf{p}_2 = (-1, 0, 0)$ GeV.

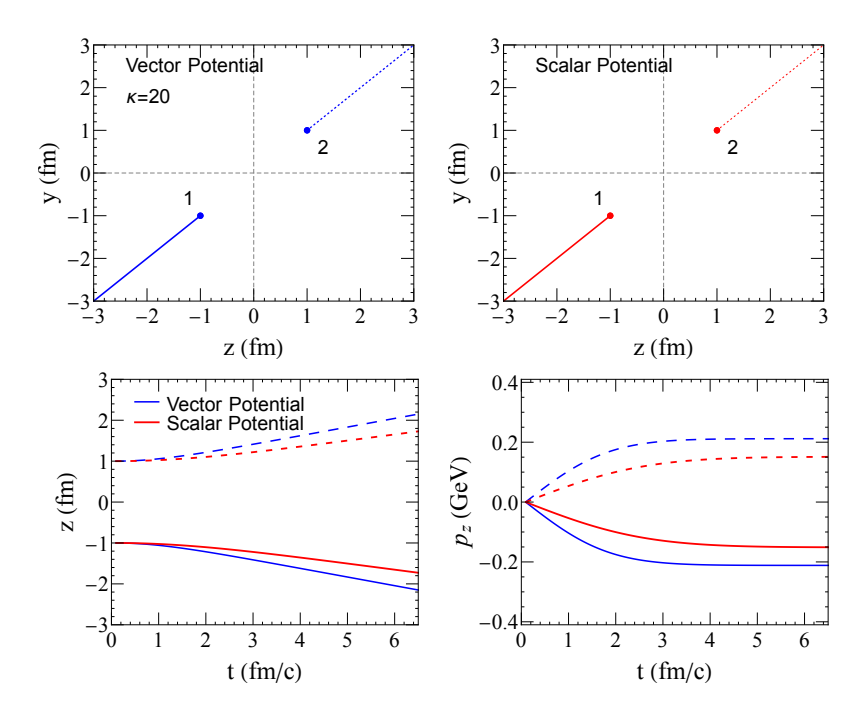


Figure 6. Time evolution of the positions and momenta of particle 1 (solid lines) and 2 (dashed lines), applying the relativistic time evolution equations. The blue line represents the time evolution with the vector potential only, the red line that with a scalar potential only. The initial condition III is chosen and with $\kappa = 20$ in the density. Here the scalar potential is multiplied by -1 to make this potential repulsive. At t = 0 $A_0 = S$ is imposed.

The initial condition III is the static case, while IV is the initial condition for a two particle scattering.

We investigate now how vector and scalar potentials influence the particle trajectories. For this purpose we study the trajectories of two particles, separately for only a vector potential or only a scalar potential and impose initially $A_0 = S$.

We start out with the initial condition III, where the particles are at rest and initially $A_0 = S \neq 0$. The initial condition $A_0 = S$ has the consequence that $H_1^A \neq H_1^S$ (Eq. (4.2)) and therefore the asymptotic momentum differs for the two cases. The different trajectories are shown in Fig. 6, top row, for $\kappa = 20$ yielding $A_0 = S = 45.83$ MeV. In the lower panel we display for the two potentials the time evolution of the position (z which is due to the initial condition = y) and the momentum p_z ($= p_y$) of both particles. Initially p_z is zero. At the beginning, the trajectories for the scalar and vector interaction are very similar, a difference emerge only when the system evolves. Particles, accelerated by the repulsive force, acquire velocity, which in turn generates finite vector components of A^{μ} . The final momentum is determined by energy conservation $H(t \to \infty) = H(t = 0)$ and is larger for a vector potential than for a scalar potential. This means that for this initial condition and $A^0(t = 0) = S(t = 0)$ initially more potential energy is stored for a vector potential than for a scalar potential, as can be also seen from Eq. (4.2).

We study now the trajectories if the particles have initially a finite momentum. Here

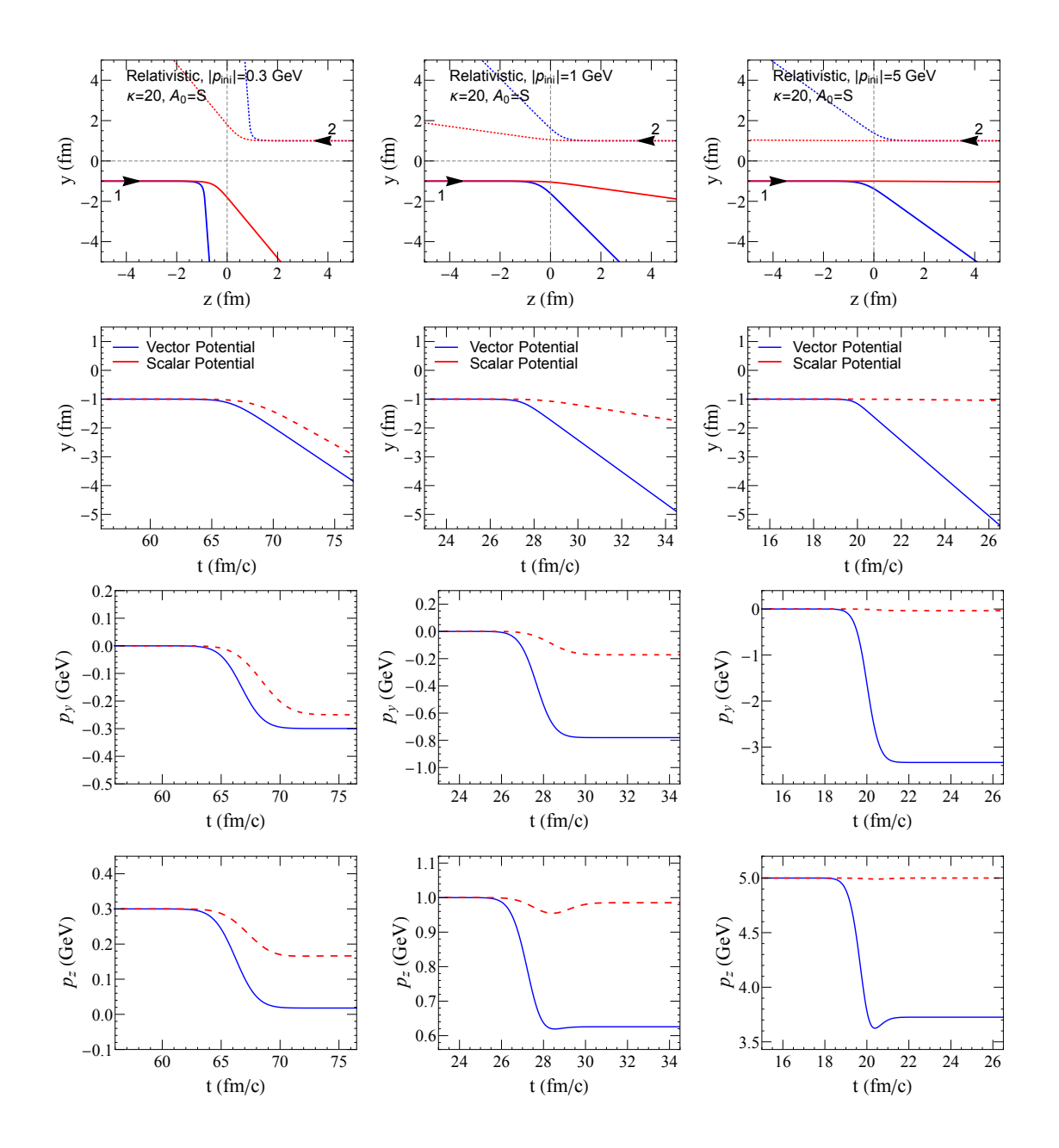


Figure 7. Comparison of the relativistic trajectories with only vector (solid color lines) and only scalar potential (dashed color lines) (see Eq. (4.35)). $A_0 = S$ is imposed. For the initial positions the initial condition IV is chosen and $\kappa = 20$, with an initial momentum $|\mathbf{p}| = 0.3$ GeV (left), $|\mathbf{p}| = 1$ GeV (middle), and $|\mathbf{p}| = 5$ GeV (right).

the trajectories obey $H^A = H^S = 0$. We apply the initial condition IV, which implies that the particles are initially not interacting and assume that $A^0 = E\rho/(1+\rho)$ and $S = m\rho$ are identical in a medium of density $\rho = 1$. Both A^0 and S depend on the momenta and positions of the two particles. This choice is made in view of the possible application of our approach to proton - heavy-ion collisions, where the analysis of the experimental data yields $A^0 \approx S$ [38]. Here we choose $\kappa = 20$ in the interaction density, Eq. (4.36), which

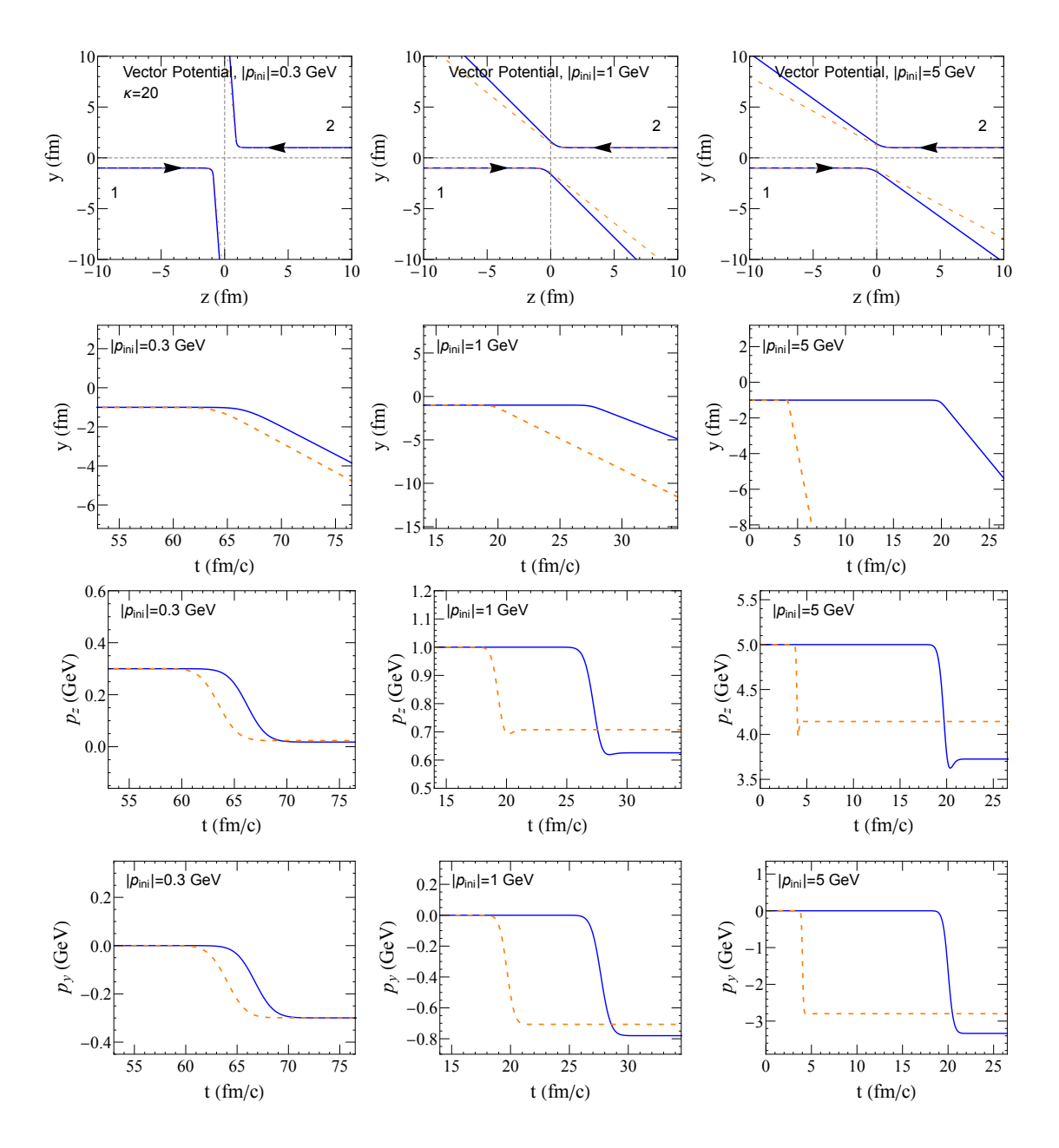


Figure 8. Comparison of the relativistic trajectories (solid color lines) to the non-relativistic trajectories (dashed color lines) with only the vector potential of Eq. (4.35). The initial condition IV is applied and $\kappa = 20$. The initial momentum is $|\mathbf{p}| = 0.3$ GeV (left), $|\mathbf{p}| = 1$ GeV (middle), and $|\mathbf{p}| = 5$ GeV (right). The bottom three panels show y, p_z , and p_y of particle 1 as a function of time applying relativistic and non-relativistic evolution equations.

gives as before $A_0 = S = 45.83$ MeV.

In Fig. 7 we display the results for an initial momentum p = 0.3 GeV (left), p = 1 GeV (middle) and p = 5 GeV (right). The first row shows the trajectories in the z - y plane, the next three rows display y(t), $p_y(t)$, and $p_z(t)$. For all initial momenta the vector potential gives a larger final p_y than the scalar potential and consequently, due to energy

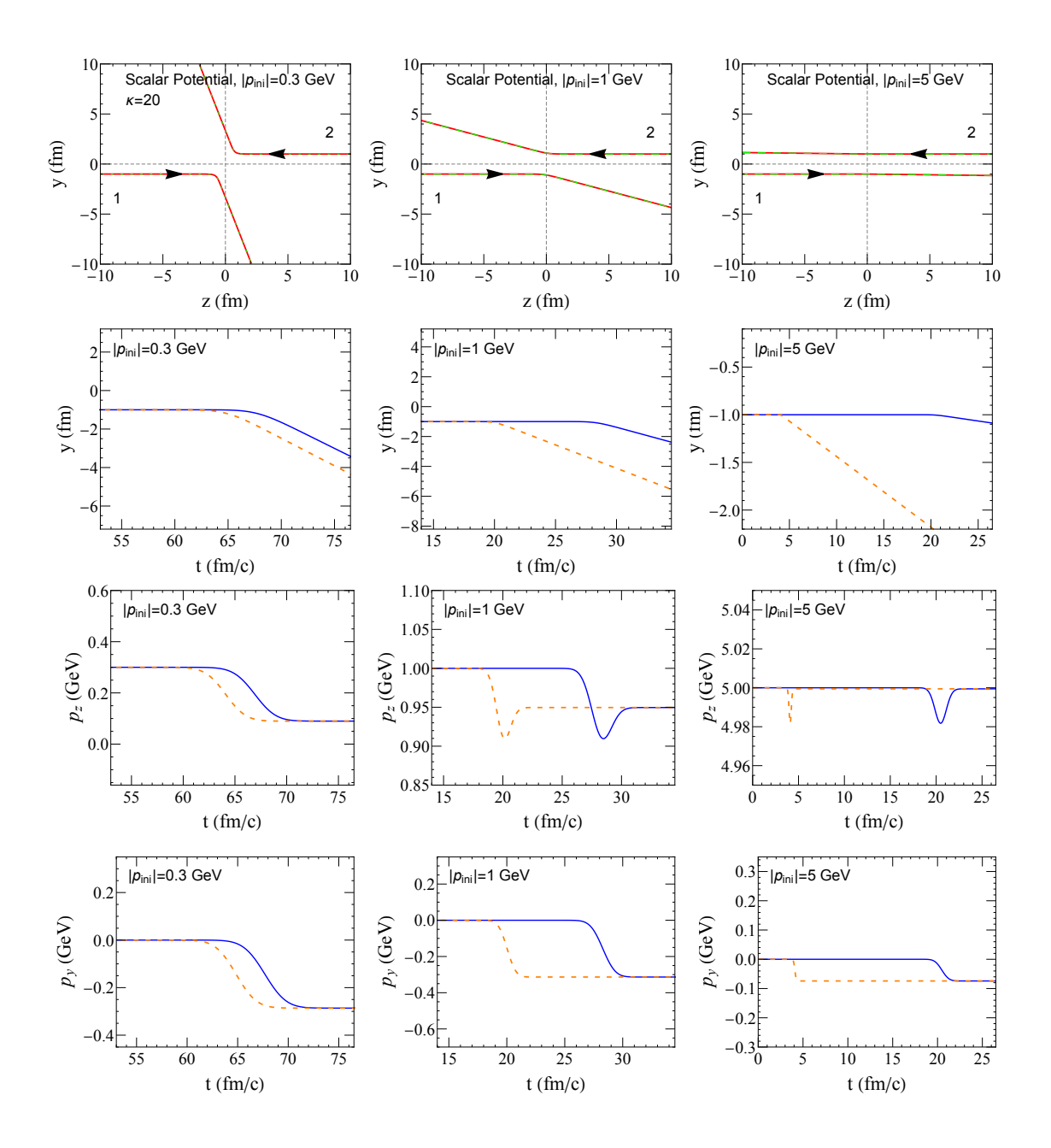


Figure 9. Same as Fig. 8 but with only the scalar potential.

conservation, a smaller p_z . Already for the non-relativistic energy ($p_z = 0.3 \text{ GeV}$, m = 1 GeV) the trajectories differ substantially because a vector potential creates a Lorentz force whereas for a scalar potential the force is given by the density gradient. The vector potential deflects the particle to almost 90° with a very small p_z left, at p = 1(5) GeV the scattering angle is $51(41^\circ)$, thus it decreases with increasing energy.

For the scalar potential the scattering angle decreases from 73° over 18° to 0.9° if the momentum increases from 0.3 to 5 GeV due to the increasingly shorter interaction time. Hence the difference of the scattering angles and the trajectories between a scalar and a

vector interaction increases with increasing initial momentum. This is due to the different mechanism which create a transverse momentum. For a scalar potential it is the gradient of the potential whereas the vector potential acts in a similar way as a Lorentz force, which is proportional to the particle velocity. By comparing the scattering angle, it decreases much faster for a scalar potential than for a vector potential.

We compare now the relativistic trajectories with their non-relativistic counterparts, in Fig. 8 for the vector potential and in Fig. 9 for the scalar potential. Again we employ the initial condition IV, $\kappa=20$ and $A^0=S$. As in the previous figure we perform these calculations for the initial momenta $p=0.3,\,1$ and 5 GeV. The non-relativistic quantities are given as dashed lines whereas the relativistic ones as solid lines. Since we describe an elastic scattering process the initial and final momentum $\sqrt{p_z^2+p_y^2}$ is identical, for the relativistic as well as for the non-relativistic case.

At p=0.3 GeV, we see a very small difference between the relativistic and non-relativistic trajectories, as expected because p/m=0.3. The main difference in the time evolution comes from the different velocities, p/m and p/E, which makes the non-relativistic particles faster. In the case of a scalar potential, the asymptotic values of the momentum for a relativistic and non-relativistic calculation are also identical at final time because the only difference in the EoMs is the velocity (or the pre-factor λ)(see Eq. (4.41) and Eq. (4.43)). For the vector potential, on the contrary, already for beam momenta of 1 GeV the momentum transfer in non-relativistic calculation is considerably smaller than in the relativistic counterpart, leading consequently to very different scattering angles.

We can conclude at already at p=1 GeV for a vector potential the non-relativistic trajectories deviate substantially from their relativistic counterparts, whereas for a scalar potential there is very little difference in the scattering angle. If we exchange the vector potential by a scalar potential the trajectories and the transverse momentum transfer changes considerably and shows a completely different systematics as a function of the beam momentum. This is of importance for the non-relativistic reduction of the relativistic potentials, the so called Schrödinger equivalent potential, in which the scalar density (on which depends S) and the vector density (on which depends S) are considered as identical.

4.5.2 The frame-independence of the trajectories

It is essential to verify also numerically that the trajectories of the particles are independent of the reference system, in which the EoMs are calculated. To demonstrate this, we compute the particle trajectories using the equations of motion (4.41) with both vector and scalar potential (Eq. (4.35) in the frame in which the initial condition is given. In the second calculation, we transform the initial condition to the center-of-mass (CoM) frame of the two-particle system and calculate the EoMs (4.41) in this frame. Finally, we transform the results from the CoM frame to the initial frame and compare the trajectories.

The results are presented in Fig. 10. As shown in the figure, the trajectories are independent of the frame in which the time evolution has been calculated, demonstrating that the particle evolution is frame-independent, as expected from our relativistic equations. This confirms the consistency and Lorentz invariance of our numerical implementation. The left figure shows the position and the middle figure the momentum of both particles as a

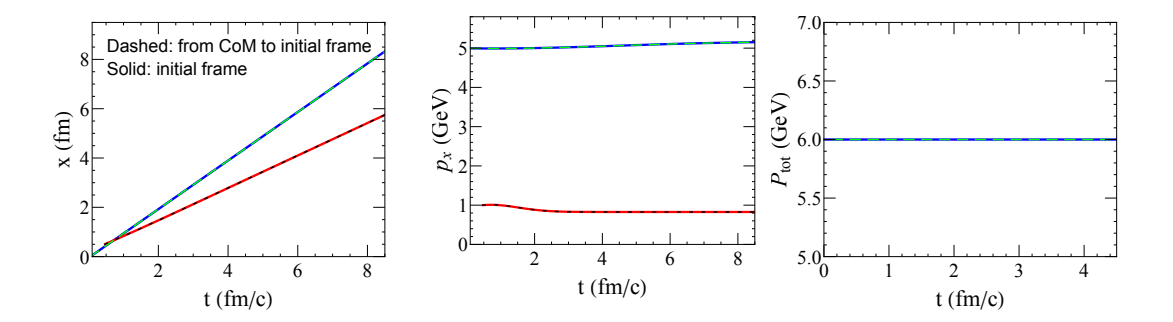


Figure 10. The positions and momenta of particle 1 (blue-solid and green-dashed lines) and 2 (red-solid and black-dashed lines) as a function of the time t applying the relativistic evolution equations. The dashed lines show the trajectory calculated first in the center-of-mass frame and then boosted to the initial frame, while the solid line shows the trajectory calculated directly in the initial frame. The initial condition I is taken and $\kappa = 1$.

function of the time t. The right figures confirms that the total momentum is conserved during the time evolution.

5 Relativistic four-body evolution

In this section, we extended the framework to four-body systems, which can be treated as a simplest symmetric "heavy-ion" collisions—deuteron-deuteron collision. This provides a simple test of relativistic dynamics beyond the two-body level and offers a pathway toward extending the framework to the N-body case. It can also serve as an additional probe of the respective roles of scalar and vector potentials in such collisions. For four interacting particles the energy constraints are

$$H_{1} = p_{1,\mu}^{*} p_{1}^{*\mu} - m_{1}^{2} + \Phi_{1},$$

$$H_{2} = p_{2,\mu}^{*} p_{2}^{*\mu} - m_{2}^{2} + \Phi_{2},$$

$$H_{3} = p_{3,\mu}^{*\mu} p_{3}^{*\mu} - m_{3}^{2} + \Phi_{3},$$

$$H_{4} = p_{4,\mu}^{*\mu} p_{4}^{*\mu} - m_{4}^{2} + \Phi_{4}.$$
(5.1)

The total Dirac Hamiltonian is $H = \lambda_1 H_1 + \lambda_2 H_2 + \lambda_3 H_3 + \lambda_4 H_4$. The conservation of each Dirac Hamiltonian H_i in time requires that the commutation relations are fulfilled, $\{H_i, H_j\} = 0$ for any i, j = 1, 2, 3, 4. The argument of the potentials Φ_i has to be a Lorentz scalar and a convenient way is to choose as an argument $q_{ij,T}^{\mu}q_{\mu ij,T}$ with

$$q_{ij,T}^{\mu} = (q_i^{\mu} - q_j^{\mu}) - \frac{(q_{i,\nu} - q_{j,\nu})P^{\nu}}{P^2}P^{\mu}, \tag{5.2}$$

where $P^{\mu} = p_1^{\mu} + p_2^{\mu} + p_3^{\mu} + p_4^{\mu}$. The time evolution equations can be extended to

$$\frac{dq_i^{\mu}}{d\tau} = \lambda_1 \{q_i^{\mu}, H_1\} + \lambda_2 \{q_i^{\mu}, H_2\} + \lambda_3 \{q_i^{\mu}, H_3\} + \lambda_4 \{q_i^{\mu}, H_4\},
\frac{dp_i^{\mu}}{d\tau} = \lambda_1 \{p_i^{\mu}, H_1\} + \lambda_2 \{p_i^{\mu}, H_2\} + \lambda_3 \{p_i^{\mu}, H_3\} + \lambda_4 \{p_i^{\mu}, H_4\}.$$
(5.3)

The four parameters λ_i are fixed by the time constraints. For the four body case, we extend the time constraints of the two-body case to

$$\chi_{1} = \frac{1}{4} (q_{1}^{\mu} - q_{2}^{\mu}) U_{\mu} = 0,$$

$$\chi_{2} = \frac{1}{4} (q_{2}^{\mu} - q_{3}^{\mu}) U_{\mu} = 0,$$

$$\chi_{3} = \frac{1}{4} (q_{3}^{\mu} - q_{4}^{\mu}) U_{\mu} - \tau = 0,$$

$$\chi_{4} = \frac{1}{4} (q_{1}^{\mu} + q_{2}^{\mu} + q_{3}^{\mu} + q_{4}^{\mu}) U_{\mu} - \tau = 0.$$
(5.4)

This means that the uniform evolution time τ in the center-of-mass frame is given by $\tau = (t_1^{com} + t_2^{com} + t_3^{com} + t_4^{com})/4$. The particle times t_1 , t_2 , t_3 , and t_4 can be reconstructed and expressed as,

$$t_{1} = \frac{1}{U^{0}}(\tau + x_{1}U_{x} + y_{1}U_{y} + z_{1}U_{z}),$$

$$t_{2} = \frac{1}{U^{0}}(\tau + x_{2}U_{x} + y_{2}U_{y} + z_{2}U_{z}),$$

$$t_{3} = \frac{1}{U^{0}}(\tau + x_{3}U_{x} + y_{3}U_{y} + z_{3}U_{z}),$$

$$t_{4} = \frac{1}{U^{0}}(\tau + x_{4}U_{x} + y_{4}U_{y} + z_{4}U_{z}).$$
(5.5)

Having the energy and time constraints we can calculate all Poisson brackets, which we show here explicitly

$$\{\chi_{1}, H_{1}\} = \frac{1}{2} U_{\mu} p_{1}^{*\nu} \left(\frac{\partial p_{1,\nu}^{*}}{\partial p_{1,\mu}} - \frac{\partial p_{1,\nu}^{*}}{\partial p_{2,\mu}} \right) + \frac{U_{\mu}}{4} \left(\frac{\partial \Phi_{1}}{\partial p_{1,\mu}} - \frac{\partial \Phi_{1}}{\partial p_{2,\mu}} \right),
\{\chi_{1}, H_{2}\} = \frac{1}{2} U_{\mu} p_{2}^{*\nu} \left(\frac{\partial p_{2,\nu}^{*}}{\partial p_{1,\mu}} - \frac{\partial p_{2,\nu}^{*}}{\partial p_{2,\mu}} \right) + \frac{U_{\mu}}{4} \left(\frac{\partial \Phi_{2}}{\partial p_{1,\mu}} - \frac{\partial \Phi_{2}}{\partial p_{2,\mu}} \right),
\{\chi_{1}, H_{3}\} = \frac{1}{2} U_{\mu} p_{3}^{*\nu} \left(\frac{\partial p_{3,\nu}^{*}}{\partial p_{1,\mu}} - \frac{\partial p_{3,\nu}^{*}}{\partial p_{2,\mu}} \right) + \frac{U_{\mu}}{4} \left(\frac{\partial \Phi_{3}}{\partial p_{1,\mu}} - \frac{\partial \Phi_{3}}{\partial p_{2,\mu}} \right),
\{\chi_{1}, H_{4}\} = \frac{1}{2} U_{\mu} p_{4}^{*\nu} \left(\frac{\partial p_{4,\nu}^{*}}{\partial p_{1,\mu}} - \frac{\partial p_{4,\nu}^{*}}{\partial p_{2,\mu}} \right) + \frac{U_{\mu}}{4} \left(\frac{\partial \Phi_{4}}{\partial p_{1,\mu}} - \frac{\partial \Phi_{4}}{\partial p_{2,\mu}} \right),
...$$

$$\{\chi_{4}, H_{1}\} = \frac{1}{2} U_{\mu} p_{1}^{*\nu} \left(\sum_{i=1}^{4} \frac{\partial p_{1,\nu}^{*}}{\partial p_{i,\mu}} \right) + \frac{U_{\mu}}{4} \sum_{i=1}^{4} \frac{\partial \Phi_{1}}{\partial p_{i,\mu}},
\{\chi_{4}, H_{2}\} = \frac{1}{2} U_{\mu} p_{2}^{*\nu} \left(\sum_{i=1}^{3} \frac{\partial p_{2,\nu}^{*}}{\partial p_{i,\mu}} \right) + \frac{U_{\mu}}{4} \sum_{i=1}^{4} \frac{\partial \Phi_{2}}{\partial p_{i,\mu}},
\{\chi_{4}, H_{3}\} = \frac{1}{2} U_{\mu} p_{3}^{*\nu} \left(\sum_{i=1}^{4} \frac{\partial p_{3,\nu}^{*}}{\partial p_{i,\mu}} \right) + \frac{U_{\mu}}{4} \sum_{i=1}^{4} \frac{\partial \Phi_{3}}{\partial p_{i,\mu}},
\{\chi_{4}, H_{4}\} = \frac{1}{2} U_{\mu} p_{3}^{*\nu} \left(\sum_{i=1}^{4} \frac{\partial p_{4,\nu}^{*}}{\partial p_{i,\mu}} \right) + \frac{U_{\mu}}{4} \sum_{i=1}^{4} \frac{\partial \Phi_{4}}{\partial p_{i,\mu}}.$$
(5.6)

Solving, as in the two body case, the eigen equation, we obtain the analytical form of the λ_i

$$\lambda_{1} = \frac{T_{1}}{2 \det [M]},$$

$$\lambda_{2} = \frac{T_{2}}{2 \det [M]},$$

$$\lambda_{3} = \frac{T_{3}}{2 \det [M]},$$

$$\lambda_{4} = \frac{T_{4}}{2 \det [M]},$$

$$(5.7)$$

where M is a 4×4 matrix with the element,

$$M_{ij} = U_{\mu} p_i^{*\nu} \frac{\partial p_{i,\nu}^*}{\partial p_{i,\mu}}, \quad i, j = 1, 2, 3, 4.$$
 (5.8)

The numerator can be expressed as,

$$T_m = \sum_{n=1}^{4} (-1)^{n+m} \det[M^{mn}] = \sum_{n=1}^{4} C_{mn},$$
(5.9)

where M^{mn} is the 3×3 matrix formed by removing row m and column n from the matrix M. We can see that C_{mn} is the cofactor matrix of M. This is the way to get the inverse matrix by definition.

Furthermore for the four-body case the EoMs can be expressed as

$$\frac{dq_i^{\mu}}{d\tau} = \sum_{k=1}^4 \lambda_k \left(2p_k^{*\nu} \frac{\partial p_{k,\nu}^*}{\partial p_i^{\mu}} \right),$$

$$\frac{dp_i^{\mu}}{d\tau} = -\sum_{k=1}^4 \lambda_k \left(2p_k^{*\nu} \frac{\partial p_{k,\nu}^*}{\partial q_i^{\mu}} + \frac{\partial \Phi_k}{\partial q_i^{\mu}} \right).$$
(5.10)

5.1 Four-nucleon system

In the following, we focus on the four nucleon system and solve the EoMs (5.10) numerically with two initial conditions:

V.
$$\mathbf{x}_1 = (-25.0, -2.0, 0) \text{ fm}, \mathbf{x}_2 = (-25.0, -1.0, 0) \text{ fm},$$

 $\mathbf{x}_3 = (25.0, 1.0, 0) \text{ fm}, \mathbf{x}_4 = (25.0, 2.0, 0) \text{ fm},$
 $\mathbf{p}_1 = (5, 0, 0) \text{ GeV}, \mathbf{p}_2 = (5, 0, 0) \text{ GeV},$
 $\mathbf{p}_3 = (-5, 0, 0) \text{ GeV}, \mathbf{p}_4 = (-5, 0, 0) \text{ GeV};$
VI. $\mathbf{x}_1 = (-25.0, -0.7, 0) \text{ fm}, \mathbf{x}_2 = (-25.0, 0.3, 0) \text{ fm},$
 $\mathbf{x}_3 = (25.0, -0.3, 0) \text{ fm}, \mathbf{x}_4 = (25.0, 0.7, 0) \text{ fm},$
 $\mathbf{p}_1 = (5, 0, 0) \text{ GeV}, \mathbf{p}_2 = (5, 0, 0) \text{ GeV},$
 $\mathbf{p}_3 = (-5, 0, 0) \text{ GeV}, \mathbf{p}_4 = (-5, 0, 0) \text{ GeV}.$

Initial condition V can be considered as vaguely as two deuterons colliding with a large impact parameter, however with the difference that the two body potential between the nucleons is always either attractive of repulsive. To clearly compare the influence of the vector and scalar potentials, we multiply the scalar potential by -1. Then, both the vector and scalar potentials are repulsive. Initial condition VI, which has a smaller impact parameter, can be considered as a collisions between two deuterons for which the impact parameter is smaller than the size of the deuteron. The interactions between nucleons are assumed to be the same as before (4.34). The results are shown in Fig. 11. The top panel,

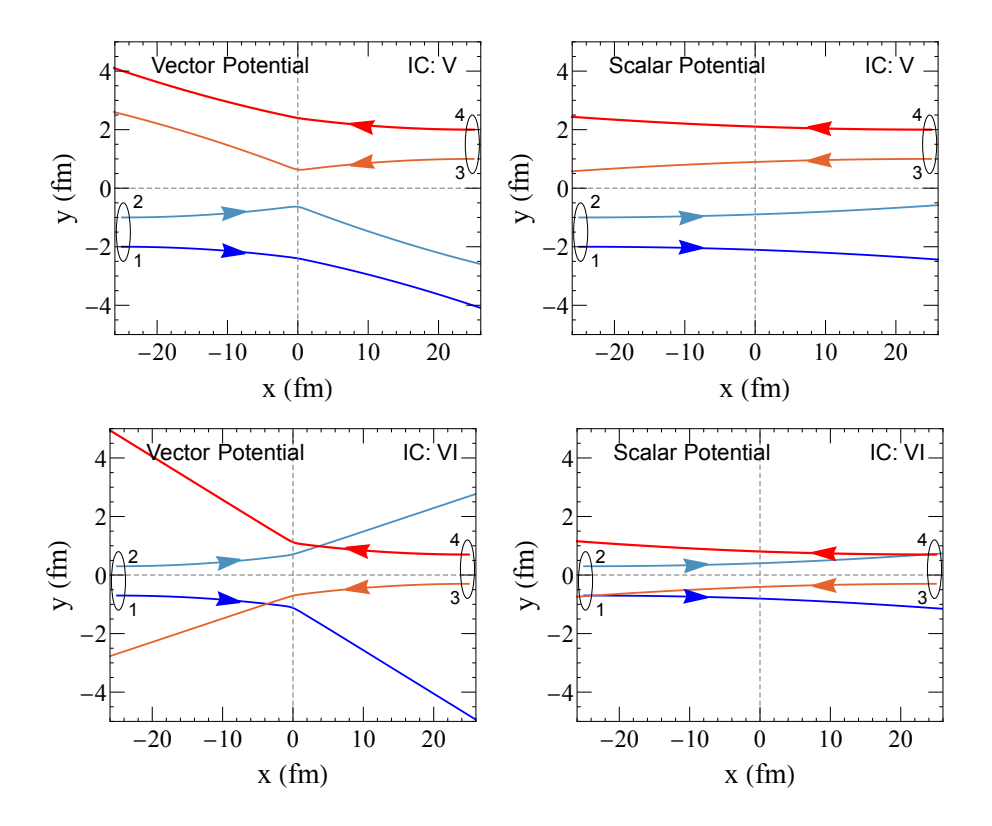


Figure 11. Time evolution of the positions and momenta of particles 1 (blue lines), 2 (dark-blue lines), 3 (dark-red line), and 4 (red line) applying the relativistic time evolution equations. The upper panel present the results for the initial condition V (IC: V), while the lower panel show that for the initial condition VI (IC: VI), and in both cases $\kappa = 1$. The left panels show the results for a vector potential and right panels that with a scalar potential but the scalar potential is multiplied by -1 to make this potential repulsive.

which shows the results of our calculation for a large impact parameter (IC: V), displays again the very different trajectories created by vector and scalar potentials, which have the same strength. Whereas for a scalar potential the repulsive interaction between the nucleons, which move into the same direction, is dominant for the trajectory, for the vector potential, due to the large relative momentum, the interaction of the particles moving in opposite direction, is equally important and leads to a large angle scattering of both "deuterons". This is also visible for central collisions (IC: VI) for which the trajectories are displayed in the bottom panel. The vector potential leads to a deflection of the nucleons

of the "deuteron" in opposite directions, what is much less the case for a scalar potential.

6 Relativistic N-body evolution

Now, we extend our approach to N-body systems. The mass shell condition yields N first-class constraints. The other N second-class constraints can be chosen as an extension of the previous two- and four-body cases. The last constraint is the only one that includes the computational time τ ,

$$\chi_{1} = \frac{1}{N} (q_{1}^{\mu} - q_{2}^{\mu}) U_{\mu} = 0,$$
...,
$$\chi_{n} = \frac{1}{N} (q_{n}^{\mu} - q_{n+1}^{\mu}) U_{\mu} = 0,$$
...,
$$\chi_{N} = \frac{1}{N} (q_{1}^{\mu} + q_{2}^{\mu} + q_{3}^{\mu} + \dots + q_{N}^{\mu}) U_{\mu} - \tau = 0.$$
(6.1)

The particle times t_i can be reconstructed,

$$t_i = \frac{1}{U_0} (\tau + x_i U_x + y_i U_y + z_i U_z). \tag{6.2}$$

With these time constraints, the Poisson brackets can be obtained as follows,

$$\{\chi_{1}, H_{1}\} = \frac{2}{N} U_{\mu} p_{1}^{*\nu} \left(\frac{\partial p_{1,\nu}^{*}}{\partial p_{1,\mu}} - \frac{\partial p_{1,\nu}^{*}}{\partial p_{2,\mu}} \right) + \frac{U_{\mu}}{N} \left(\frac{\partial \Phi_{1}}{\partial p_{1,\mu}} + \frac{\partial \Phi_{1}}{\partial p_{2,\mu}} \right),
\{\chi_{1}, H_{2}\} = \frac{2}{N} U_{\mu} p_{1}^{*\nu} \left(\frac{\partial p_{2,\nu}^{*}}{\partial p_{1,\mu}} - \frac{\partial p_{2,\nu}^{*}}{\partial p_{2,\mu}} \right) + \frac{U_{\mu}}{N} \left(\frac{\partial \Phi_{2}}{\partial p_{1,\mu}} - \frac{\partial \Phi_{2}}{\partial p_{2,\mu}} \right),
\dots,
\{\chi_{1}, H_{N}\} = \frac{2}{N} U_{\mu} p_{N}^{*\nu} \left(\frac{\partial p_{N,\nu}^{*}}{\partial p_{1,\mu}} - \frac{\partial p_{N,\nu}^{*}}{\partial p_{2,\mu}} \right) + \frac{U_{\mu}}{N} \left(\frac{\partial \Phi_{N}}{\partial p_{1,\mu}} - \frac{\partial \Phi_{N}}{\partial p_{2,\mu}} \right),
\dots,
\{\chi_{n}, H_{m}\} = \frac{2}{N} U_{\mu} p_{m}^{*\nu} \left(\frac{\partial p_{m,\nu}^{*}}{\partial p_{n,\mu}} - \frac{\partial p_{m,\nu}^{*}}{\partial p_{n+1,\mu}} \right) + \frac{U_{\mu}}{N} \left(\frac{\partial \Phi_{m}}{\partial p_{n,\mu}} - \frac{\partial \Phi_{m}}{\partial p_{n+1,\mu}} \right),
\dots,
\{\chi_{N}, H_{1}\} = \frac{2}{N} U_{\mu} p_{N}^{*\nu} \left(\sum_{i=1}^{N} \frac{\partial p_{1,\nu}^{*}}{\partial p_{i,\mu}} \right) + \frac{U_{\mu}}{N} \sum_{i=1}^{N} \frac{\partial \Phi_{i}}{\partial p_{i,\mu}},
\dots,
\{\chi_{N}, H_{N}\} = \frac{2}{N} U_{\mu} p_{N}^{*\nu} \left(\sum_{i=1}^{N} \frac{\partial p_{N,\nu}^{*}}{\partial p_{i,\mu}} \right) + \frac{U_{\mu}}{N} \sum_{i=1}^{N} \frac{\partial \Phi_{i}}{\partial p_{i,\mu}}.$$
(6.3)

We generalized the formula for λ_i to the N-body system as

$$\lambda_{1} = \frac{T_{1}}{2 \det [M]},$$
...,
$$\lambda_{N} = \frac{T_{N}}{2 \det [M]},$$
(6.4)

where M is a $N \times N$ matrix with the element,

$$M_{ij} = U_{\mu} p_i^{*\nu} \frac{\partial p_{i,\nu}^*}{\partial p_{j,\mu}}, \quad i, j = 1, ..., N.$$
 (6.5)

The numerator of λ_m can be expressed as

$$T_m = \sum_{n=1}^{N} C_{mn},\tag{6.6}$$

where C_{mn} is the cofactor matrix of matrix M.

The EoM for the N-body system can be expressed as,

$$\frac{dq_i^{\mu}}{d\tau} = \sum_{k=1}^{N} \lambda_k \left(2p_k^{*\nu} \frac{\partial p_{k,\nu}^*}{\partial p_i^{\mu}} \right),$$

$$\frac{dp_i^{\mu}}{d\tau} = -\sum_{k=1}^{N} \lambda_k \left(2p_k^{*\nu} \frac{\partial p_{k,\nu}^*}{\partial q_{i,\mu}} + \frac{\partial \Phi_k}{\partial q_i^{\mu}} \right).$$

This equation can be applied directly in a microscopic framework to describe the time evolution of a many-particle system. The details of the algorithm used to compute the above derivatives are shown in the Appendix. B.

7 Summary

In this work we derived for the first time the relativistic Molecular Dynamics for an N-body system that interacts with both scalar and vector potentials without any approximations. Our formulation addressed several fundamental challenges in relativistic many-body dynamics. In particular, we examined the implications of different choices of time constraints, analyzed the non-relativistic limit of the derived equations, tested the frame independence of the system evolution, and disentangled the distinct dynamical roles of scalar and vector potentials in scattering processes. These aspects are investigated in detail for two- and four-body systems. Finally, we present the general form of the equation of motion (EoM) for a N-body system. Looking ahead, this framework will provide the basis for studying the evolution of heavy quarks and quarkonia in a quark–gluon plasma as well as the dynamics of nucleons in medium and high energy heavy-ion collisions, where vector and scalar interaction play a quite different role and non relativistic approximations are questionable. This we will address in upcoming publications.

Acknowledgement: We acknowledge support by the Deutsche Forschungsgemeinschaft (DFG, German Research Foundation) grant BL982-3, the European Union's Horizon 2020 research and innovation program under grant agreement STRONG – 2020 - No 824093, Helmholtz Research Academy Hessen for FAIR (HFHF).

A Time constraints and relativistic kinematics

Time is not universal in relativistic mechanics. Each particle has its own time (own clock), the forth component of its position vector. For many particle systems the clock times of the different particles have to be correlated by time constraints. To discuss the influence of the time constraints on the EoMs, we take as an example the time evolution of one particle.

A.1 Time constraints

We study here 2 different time constraints and their influence on the equations of motion and on the trajectories of the particle $\mathbf{x}(t)$, the vector component as a function of the zero component of the position 4-vector. We start with the (Lorentz invariant) time constraint

$$\chi = q^{\mu}u_{\mu} - \tau = 0. \tag{A.1}$$

For the differential quantity $d\tau$ this constraint yields

$$d\tau = \gamma(dt - (d\mathbf{q})\mathbf{v}) = \gamma dt(1 - \mathbf{v}^2) = \frac{1}{\gamma}dt.$$
 (A.2)

 u^{μ} is defined as $p_{\mu}/\sqrt{p_{\nu}p^{\nu}}=p_{\mu}/m=\gamma(1,\mathbf{v})$. Taking it into Eq. (2.13) yields the EoMs,

$$\frac{dq^{\mu}}{d\tau} = \frac{p^{\mu}}{p^{\mu}u_{\mu}} = \frac{p^{\mu}}{m},$$

$$\frac{dp^{\mu}}{d\tau} = 0.$$
(A.3)

Another choice, which is discussed in the literature [48] is the non-relativistic time constraint

$$\chi = q_0 - \tau = t - \tau = 0. \tag{A.4}$$

This time constraint obeys the world line condition for the N-body case without interaction but not for an interacting system [48]. This time constraint leads directly to the EoMs

$$\frac{dq^{\mu}}{d\tau} = \frac{dq^{\mu}}{dt} = \frac{p^{\mu}}{p_0},$$

$$\frac{dp^{\mu}}{d\tau} = \frac{dp^{\mu}}{dt} = 0,$$
(A.5)

which are not Lorentz invariant, because p^{μ}/p_0 is no quantity which can be Lorentz transformed.

Even covariant time constraints are not unique. For example,

$$\chi = 2q^{\mu}U_{\mu} - \tau = 0 \tag{A.6}$$

also fulfills the requirement of a time constraint to connect in a Lorentz invariant way the dt with $d\tau$. This choice gives $\frac{dq^{\mu}}{d\tau} = \frac{p^{\mu}}{2p^{\mu}U_{\mu}} = \frac{p^{\mu}}{2m}$ and therefore not, as we will see, the right non-relativistic limit. For the time evolution of more than one particles there are, however, several forms of time constraints, which give the right non-relativistic limit. Therefore the

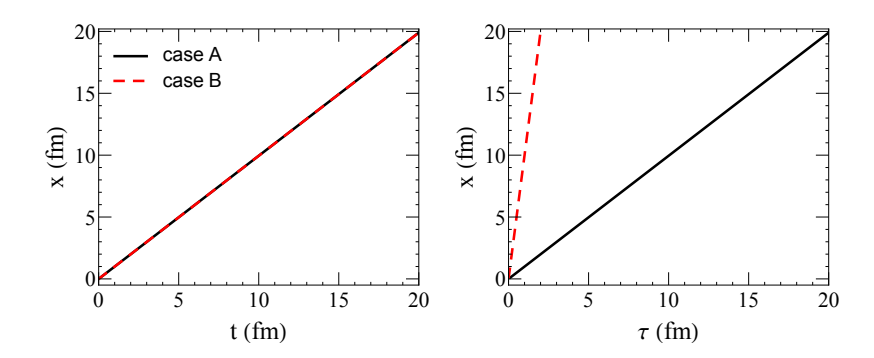


Figure 12. Trajectories in two cases with the time t and the computational time τ .

time evolution of a relativistic many-body system is not completely determined without fixing the time constraints.

Let us now examine the trajectories obtained from the two EoMs Eqs. (A.5) (called case A) and (A.3) (called case B). For case A we find

$$x^{\mu} = x_0^{\mu} + \frac{p^{\mu}}{p^0}\tau,\tag{A.7}$$

whereas case B yields

$$x^{\mu} = x_0^{\mu} + \frac{p^{\mu}}{m}\tau. \tag{A.8}$$

As a function of τ the trajectories are rather different but for $\mathbf{x}(t)$, where t is the zero component of x^{μ} we find identical trajectories. This is shown in Fig. 12. The calculation is performed with the initial position x = y = z = 0 at $\tau_0 = 0$, and the initial momentum is chosen as $p_x = 10$ GeV, $p_y = p_z = 0$, and the particle mass is m = 1 GeV. This demonstrates that the trajectory itself does not change under different time constraints.

A.2 Standard derivation of relativisitic EoMs

It is worthwhile to connect these constraints to the EoMs derived in textbooks for the relativistic kinematics. The non-relativistic equations of motion are given by

$$\frac{d\mathbf{q}}{dt} = \frac{\mathbf{p}}{m} = \mathbf{v},$$

$$\frac{d\mathbf{p}}{dt} = 0.$$
(A.9)

To construct 4-vector one extends the three-vectors to the position and momentum 4-vectors. In an arbitrary reference system the particle position and momentum is expressed by the 4-vector $q^{\mu} = (q^0, \mathbf{q})$ and $p^{\mu} = (p^0, \mathbf{p})$ with $q^0 = t$ and $p^0 = \sqrt{m^2 + \mathbf{p}^2}$.

Using the relativistic relations $\mathbf{p}=\gamma m\mathbf{v}$ and $p_0=\gamma m$ the first equation can be rewritten as

$$\frac{d\mathbf{q}}{dt} = \mathbf{v} = \frac{\mathbf{p}}{p_0}.\tag{A.10}$$

Including the forth components, we obtain the same EoMs as for the non covariant time constraint, Eq. (A.5). It describes the time evolution, seen from a system with respect to which the particle has a velocity \mathbf{p}/p_0 . To make them invariant we introduce the scalar quantity

$$(d\tau)^2 = dx_\mu dx^\mu = (\frac{1}{\gamma} dt)^2 \underbrace{=}_{\text{particle rest system}} (dt)^2, \tag{A.11}$$

which is the infinitesimal time in the particle rest system. This relation is identical to relativistic time constraint, Eq. (A.1). Replacing dt by $d\tau$, Eq. (A.10) reads as

$$\frac{d\mathbf{q}}{d\tau} = \gamma \mathbf{v} = \mathbf{u} = \frac{\mathbf{p}}{m},\tag{A.12}$$

where \mathbf{u} are the vector components of the velocity 4-vector $u^{\mu} = \gamma(1, \mathbf{v})$ and $p^{\mu} = mu^{\mu}$. Including the zero components we have then the time evolution equations, Eqs. (A.3), which are covariant. We can therefore conclude that the relativistic EoMs, which we apply in the relativistic constraint dynamics, can be related to the standard results obtained in relativistic kinematics.

B Numerical method for computing the mechanical momentum and related derivatives

For nuclear systems, the interaction involve both the vector and scalar potential, as shown in Eq. (4.34). The vector potential is given by

$$A_i^{\mu} = \sum_{j \neq i}^{N} p_j^{*\mu} \rho_{ij}(q_T), \quad i = 1, ..., N,$$
(B.1)

where $p_j^{*\mu} = p_j^{\mu} - A_j^{\mu}$. Aiming at calculating the equations of motion and the parameters λ_i , one need the explicit form of the mechanical momentum p_i^* for N-bodies. The above equation can be written as,

$$A_i^{\mu} + \sum_{j \neq i}^{N} A_j^{\mu} \rho_{ij} = \sum_{j \neq i}^{N} p_j^{\mu} \rho_{ij}$$
 (B.2)

or converted into a matrix form,

$$\mathbf{D} \cdot \mathbf{A} = \mathbf{b},\tag{B.3}$$

where $\mathbf{A} = (A_1, ..., A_N)^T$. The vector $\mathbf{b} = (b_1, ..., b_N)^T$ with components $b_i = \sum_{j \neq i}^N p_j^{\mu} \rho_{ij}$. \mathbf{D} is a $N \times N$ symmetric matrix with $D_{ii} = 1$ and $D_{ij} = D_{ji} = \rho_{ij}$ for $i \neq j$. Therefore, the vector potential can be obtained as,

$$\mathbf{A} = \mathbf{D}^{-1} \cdot \mathbf{b}. \tag{B.4}$$

The mechanical momentum is $p_i^{*\mu} = p_i^{\mu} - A_i^{\mu}$. Now we just need to calculate the inverse of the matrix **D**, which is related to the interaction density.

With A^{μ} , we can further calculate the other two derivatives. The first one is,

$$\frac{\partial p_{i,\nu}^*}{\partial p_{j,\mu}} = \delta_{ij} \delta_{\nu}^{\mu} - \frac{\partial A_{i,\nu}}{\partial p_{j,\mu}}
= \delta_{ij} \delta_{\nu}^{\mu} - \sum_{k} (D^{-1})_{ik} \frac{\partial b_{k,\nu}}{\partial p_{j,\mu}}.$$
(B.5)

From the definition of b_i , we have,

$$\frac{\partial b_{k,\nu}}{\partial p_{j,\mu}} = \sum_{l \neq k} \delta_{lj} \delta^{\mu}_{\nu} \rho_{kl}. \tag{B.6}$$

The derivation with respect to the coordinates is given by

$$\frac{\partial p_{i,\nu}^*}{\partial q_{j,\mu}} = -\frac{\partial A_{i,\nu}}{\partial q_{j,\mu}} = \sum_{m,n} (D^{-1})_{im} \frac{\partial D_{mn}}{\partial q_{j,\mu}} A_{n,\nu} - \sum_{k} (D^{-1})_{ik} \frac{\partial b_{k,\nu}}{\partial q_{j,\mu}},\tag{B.7}$$

where

$$\frac{\partial b_{k,\nu}}{\partial q_{j,\mu}} = \sum_{l \neq k} p_{l,\nu} \frac{\partial \rho_{kl}}{\partial q_{j,\mu}} = \sum_{l \neq k} p_{l,\nu} (\delta_{jk} - \delta_{jl}) \frac{\partial \rho_{kl}}{\partial (q_k - q_l)_{\mu}}.$$
 (B.8)

References

- [1] P. Danielewicz, Quantum Theory of Nonequilibrium Processes. 1., Annals Phys. 152 (1984) 239–304.
- [2] G. F. Bertsch and S. Das Gupta, A Guide to microscopic models for intermediate-energy heavy ion collisions, Phys. Rept. **160** (1988) 189–233.
- [3] W. Botermans and R. Malfliet, Quantum transport theory of nuclear matter, Phys. Rept. 198 (1990) 115–194.
- [4] W. Cassing, V. Metag, U. Mosel, and K. Niita, Production of energetic particles in heavy ion collisions, Phys. Rept. 188 (1990) 363–449.
- [5] A. Bonasera, F. Gulminelli, and J. Molitoris, *The Boltzmann equation at the borderline: a decade of Monte Carlo simulations of a quantum kinetic equation*, Phys. Rept. **243** (1994) 1–124.
- [6] W. Cassing and E. L. Bratkovskaya, *Hadronic and electromagnetic probes of hot and dense nuclear matter*, Phys. Rept. **308** (1999) 65–233.
- [7] J. Xu, Transport approaches for the description of intermediate-energy heavy-ion collisions, Prog. Part. Nucl. Phys. **106** (2019) 312–359, [arXiv:1904.00131].
- [8] **TMEP** Collaboration, J. Xu et al., Understanding transport simulations of heavy-ion collisions at 100A and 400A MeV: Comparison of heavy-ion transport codes under controlled conditions, Phys. Rev. C **93** (2016) 044609, [arXiv:1603.08149].
- [9] TMEP Collaboration, H. Wolter et al., Transport model comparison studies of intermediate-energy heavy-ion collisions, Prog. Part. Nucl. Phys. 125 (2022) 103962, [arXiv:2202.06672].

- [10] M. Bleicher and E. Bratkovskaya, Modelling relativistic heavy-ion collisions with dynamical transport approaches, Prog. Part. Nucl. Phys. 122 (2022) 103920.
- [11] W. Cassing, Quantum correlation dynamics and in-medium 3↔3 collisions of fermions, Phys. Rev. C 112 (2025) 024601, [arXiv:2505.21683].
- [12] W. Cassing, Transport Theories for Strongly-Interacting Systems: Applications to Heavy-Ion Collisions, Lect. Notes Phys. **989** (2021) pp.
- [13] W. Cassing, Anti-baryon production in hot and dense nuclear matter, Nucl. Phys. A 700 (2002) 618–646, [nucl-th/0105069].
- [14] W. Cassing and S. Juchem, Semiclassical transport of particles with dynamical spectral functions, Nucl. Phys. A 665 (2000) 377–400, [nucl-th/9903070].
- [15] W. Cassing and S. Juchem, Semiclassical transport of hadrons with dynamical spectral functions in A + A collisions at SIS / AGS energies, Nucl. Phys. A 672 (2000) 417–445, [nucl-th/9910052].
- [16] W. Cassing and E. L. Bratkovskaya, Parton transport and hadronization from the dynamical quasiparticle point of view, Phys. Rev. C 78 (2008) 034919, [arXiv:0808.0022].
- [17] P. Moreau, O. Soloveva, L. Oliva, T. Song, W. Cassing, and E. Bratkovskaya, Exploring the partonic phase at finite chemical potential within an extended off-shell transport approach, Phys. Rev. C 100 (2019) 014911, [arXiv:1903.10257].
- [18] P. Danielewicz and G. F. Bertsch, Production of deuterons and pions in a transport model of energetic heavy ion reactions, Nucl. Phys. A 533 (1991) 712–748.
- [19] C. M. Ko, Q. Li, and R.-C. Wang, Relativistic Vlasov Equation for Heavy Ion Collisions, Phys. Rev. Lett. 59 (1987) 1084–1087.
- [20] B.-A. Li, L.-W. Chen, and C. M. Ko, Recent Progress and New Challenges in Isospin Physics with Heavy-Ion Reactions, Phys. Rept. 464 (2008) 113–281, [arXiv:0804.3580].
- [21] O. Buss, T. Gaitanos, K. Gallmeister, H. van Hees, M. Kaskulov, O. Lalakulich, A. B. Larionov, T. Leitner, J. Weil, and U. Mosel, Transport-theoretical Description of Nuclear Reactions, Phys. Rept. 512 (2012) 1–124, [arXiv:1106.1344].
- [22] **SMASH** Collaboration, J. Weil et al., Particle production and equilibrium properties within a new hadron transport approach for heavy-ion collisions, Phys. Rev. C **94** (2016) 054905, [arXiv:1606.06642].
- [23] M. Kim, S. Jeon, Y.-M. Kim, Y. Kim, and C.-H. Lee, Extended parity doublet model with a new transport code, Phys. Rev. C 101 (2020) 064614, [arXiv:2006.02023].
- [24] Z.-W. Lin, C. M. Ko, B.-A. Li, B. Zhang, and S. Pal, A Multi-phase transport model for relativistic heavy ion collisions, Phys. Rev. C 72 (2005) 064901, [nucl-th/0411110].
- [25] Z. Xu and C. Greiner, Thermalization of gluons in ultrarelativistic heavy ion collisions by including three-body interactions in a parton cascade, Phys. Rev. C 71 (2005) 064901, [hep-ph/0406278].
- [26] A. Raab Chem. Phys. Lett. 319 (2000) 674.
- [27] J. Broeckhove, L. Lathouwers, E. Kesteloot, and P. Van Leuven, On the equivalence of time-dependent variational principles, Chem. Phys. Lett. 149 (1988) 547–550.
- [28] H. Sorge, H. Stoecker, and W. Greiner, Poincare Invariant Hamiltonian Dynamics: Modeling Multi - Hadronic Interactions in a Phase Space Approach, Annals Phys. 192 (1989) 266–306.

- [29] T. Maruyama, S. W. Huang, N. Ohtsuka, G.-Q. Li, A. Faessler, and J. Aichelin, Lorentz covariant description of intermediate-energy heavy ion reactions in relativistic quantum molecular dynamics, <u>Nucl. Phys. A</u> 534 (1991) 720–740.
- [30] E. Lehmann, R. K. Puri, A. Faessler, T. Maruyama, G.-Q. Li, N. Ohtsuka, S. W. Huang, D. T. Khoa, and M. A. Matin, Relativistic versus nonrelativistic quantum molecular dynamics, Prog. Part. Nucl. Phys. 30 (1993) 219–228.
- [31] Y. Nara, N. Otuka, A. Ohnishi, K. Niita, and S. Chiba, Study of relativistic nuclear collisions at AGS energies from p + Be to Au + Au with hadronic cascade model, Phys. Rev. C 61 (2000) 024901, [nucl-th/9904059].
- [32] Y. Nara and H. Stoecker, Sensitivity of the excitation functions of collective flow to relativistic scalar and vector meson interactions in the relativistic quantum molecular dynamics model RQMD.RMF, Phys. Rev. C 100 (2019) 054902, [arXiv:1906.03537].
- [33] Y. Nara, A. Jinno, T. Maruyama, K. Murase, and A. Ohnishi, Poincaré covariant cascade method for high-energy nuclear collisions, Phys. Rev. C 108 (2023) 024910, [arXiv:2306.12131].
- [34] Y. Nara, T. Maruyama, and H. Stoecker, Momentum-dependent potential and collective flows within the relativistic quantum molecular dynamics approach based on relativistic mean-field theory, Phys. Rev. C 102 (2020) 024913, [arXiv:2004.05550].
- [35] S. A. Bass et al., Microscopic models for ultrarelativistic heavy ion collisions, Prog. Part. Nucl. Phys. 41 (1998) 255–369, [nucl-th/9803035].
- [36] M. Bleicher et al., Relativistic hadron hadron collisions in the ultrarelativistic quantum molecular dynamics model, J. Phys. G 25 (1999) 1859–1896, [hep-ph/9909407].
- [37] R. Marty and J. Aichelin, Molecular dynamics description of an expanding q/q̄ plasma with the Nambu–Jona-Lasinio model and applications to heavy ion collisions at energies available at the BNL Relativistic Heavy Ion Collider and the CERN Large Hadron Collider, Phys. Rev. C 87 (2013) 034912, [arXiv:1210.3476].
- [38] E. D. Cooper, S. Hama, B. C. Clark, and R. L. Mercer, Global Dirac phenomenology for proton nucleus elastic scattering, Phys. Rev. C 47 (1993) 297–311.
- [39] J. D. Walecka, A Theory of highly condensed matter, Annals Phys. 83 (1974) 491–529.
- [40] J. Boguta and A. R. Bodmer, Relativistic Calculation of Nuclear Matter and the Nuclear Surface, Nucl. Phys. A 292 (1977) 413–428.
- [41] P. G. Reinhard, The Relativistic Mean Field Description of Nuclei and Nuclear Dynamics, Rept. Prog. Phys. 52 (1989) 439.
- [42] B. D. Serot and J. D. Walecka, Recent progress in quantum hadrodynamics, <u>Int. J. Mod. Phys. E</u> 6 (1997) 515–631, [nucl-th/9701058].
- [43] P. A. M. Dirac, Forms of Relativistic Dynamics, Rev. Mod. Phys. 21 (1949) 392–399.
- [44] A. Komar, Constraint Formalism of Classical Mechanics, Phys. Rev. D 18 (1978) 1881–1886.
- [45] A. Komar, Interacting Relativistic Particles, Phys. Rev. D 18 (1978) 1887–1893.
- [46] J. Samuel, Relativistic Particle Models With Separable Interactions, Phys. Rev. D 26 (1982) 3482.
- [47] J. Samuel, Constraints in Relativistic Hamiltonian Mechanics, Phys. Rev. D 26 (1982) 3475.

- [48] E. C. G. Sudarshan, N. Mukunda, and J. N. Goldberg, Constraint Dynamics of Particle World Lines, Phys. Rev. D 23 (1981) 2218.
- [49] P. P. Fiziev and I. T. Todorov, Effective one-body approach to the relativistic two-body problem, Phys. Rev. D **63** (2001) 104007, [gr-qc/0010104].
- [50] H. Sorge, H. Stoecker, and W. Greiner, RELATIVISTIC QUANTUM MOLECULAR DYNAMICS APPROACH TO NUCLEAR COLLISIONS AT ULTRARELATIVISTIC ENERGIES, Nucl. Phys. A 498 (1989) 567C-576C.
- [51] C. Fuchs, E. Lehmann, L. Sehn, F. Scholz, T. Kubo, J. Zipprich, and A. Faessler, Heavy ion collisions and the density dependence of the local mean field, <u>Nucl. Phys. A</u> 603 (1996) 471–485.
- [52] A. Kihlberg, R. Marnelius, and N. Mukunda, Relativistic Potential Models as Systems With Constraints and Their Interpretation, Phys. Rev. D 23 (1981) 2201.
- [53] P. Hillmann, J. Steinheimer, and M. Bleicher, Directed, elliptic and triangular flow of protons in Au+Au reactions at 1.23 A GeV: a theoretical analysis of the recent HADES data, <u>J.</u> Phys. G 45 (2018) 085101, [arXiv:1802.01951].
- [54] J. Aichelin and H. Stoecker, Quantum molecular dynamics. A Novel approach to N body correlations in heavy ion collisions, Phys. Lett. B 176 (1986) 14–19.
- [55] C. Hartnack, Z. X. Li, L. Neise, G. Peilert, A. Rosenhauer, H. Sorge, H. Stoecker, W. Greiner, and J. Aichelin, Quantum Molecular Dynamics: A Microscopic Model From Unilac to CERN Energies, Nucl. Phys. A 495 (1989) 303C–320C.
- [56] J. Aichelin, 'Quantum' molecular dynamics: A Dynamical microscopic n body approach to investigate fragment formation and the nuclear equation of state in heavy ion collisions, Phys. Rept. 202 (1991) 233–360.
- [57] J. Aichelin, E. Bratkovskaya, A. Le Fèvre, V. Kireyeu, V. Kolesnikov, Y. Leifels, V. Voronyuk, and G. Coci, Parton-hadron-quantum-molecular dynamics: A novel microscopic n -body transport approach for heavy-ion collisions, dynamical cluster formation, and hypernuclei production, Phys. Rev. C 101 (2020) 044905, [arXiv:1907.03860].